

1 **Quantifying atmospheric nitrogen deposition through a nationwide monitoring**
2 **network across China**

3 W. Xu¹, X. S. Luo^{1,2}, Y. P. Pan³, L. Zhang⁴, A. H. Tang¹, J. L. Shen⁵, Y. Zhang⁶, K. H. Li⁷, Q. H.
4 Wu¹, D. W. Yang¹, Y. Y. Zhang¹, J. Xue¹, W. Q. Li⁸, Q. Q. Li^{1,9}, L. Tang⁹, S. H. Lu¹⁰, T. Liang¹¹, Y.
5 A. Tong¹¹, P. Liu¹², Q. Zhang¹², Z. Q. Xiong¹³, X. J. Shi¹⁴, L. H. Wu¹⁵, W. Q. Shi¹⁶, K. Tian¹⁷, X. H.
6 Zhong¹⁷, K. Shi¹⁸, Q. Y. Tang¹⁹, L. J. Zhang²⁰, J. L. Huang²¹, C. E. He²², F. H. Kuang²³, B. Zhu²³,
7 H. Liu²⁴, X. Jin²⁵, Y. J. Xin²⁵, X. K. Shi²⁶, E. Z. Du²⁷, A. J. Dore²⁸, S. Tang²⁸, J. L. Jr. Collett²⁹, K.
8 Goulding³⁰, Y. X. Sun³¹, J. Ren³², F. S. Zhang¹, X. J. Liu^{1,*}

9 ¹College of Resources and Environmental Sciences, China Agricultural University, Beijing
10 100193, China

11 ²Institute of Plant Nutrition, Resources and Environmental Sciences, Henan Academy of
12 Agricultural Sciences, Zhengzhou 450002, China

13 ³State Key Laboratory of Atmospheric Boundary Layer Physics and Atmospheric Chemistry
14 (LAPC), Institute of Atmospheric Physics, Chinese Academy of Sciences, Beijing 100029, China

15 ⁴Laboratory for Climate and Ocean-Atmosphere Studies, Department of Atmospheric and Oceanic
16 Sciences, School of Physics, Peking University, Beijing 100871, China

17 ⁵Institute of Subtropical Agriculture, Chinese Academy of Sciences, Changsha 4410125, China

18 ⁶College of Nature Conservation, Beijing Forestry University, Beijing 100083, China

19 ⁷Xinjiang Institute of Ecology and Geography, Chinese Academy of Sciences, Urumqi 830011,
20 China

21 ⁸Fujian Institute of Tobacco Agricultural Sciences, Fuzhou 350003, China

22 ⁹College of Resources and Environmental Sciences, Yunnan Agricultural University, Kunming
23 650224, China

24 ¹⁰Soil and Fertilizer Institute, Sichuan Academy of Agricultural Sciences, Chengdu 610066, China

25 ¹¹Nature Resource and Environment College, Northwest A&F University, Yangling
26 712100, China

27 ¹²Institute of Agricultural Environment and Resource, Shanxi Academy of Agricultural Sciences,
28 Taiyuan 030031, China

29 ¹³College of Resources and Environmental Sciences, Nanjing Agricultural University, Nanjing
30 210009, China

31 ¹⁴College of Resources and Environment, Southwest University, Chongqing 400716, China

32 ¹⁵College of Environmental and Resource Sciences, Zhejiang University, Hangzhou 310029,
33 China

34 ¹⁶South Subtropical Crops Research Institute, Chinese Academy of Tropical Agricultural Science,
35 Zhanjiang 524091, China

36 ¹⁷Rice Research Institute, Guangdong Academy of Agricultural Sciences, Guangzhou 510640,
37 China

38 ¹⁸College of Environmental and Chemical Engineering, Dalian Jiaotong University, Dalian

39 116028, China

40 ¹⁹College of Agriculture, Hunan Agricultural University, Changsha 410128, China

41 ²⁰College of Resources and Environment, Agricultural University of Hebei, Baoding 071001,
42 China

43 ²¹College of Plant Science and Technology, Huazhong Agricultural University, Wuhan, China

44 ²²Institute of Geographic Sciences and Natural Resources, Chinese Academy of Sciences, Bei
45 jing 100101, China

46 ²³Institute of Mountain, Hazards and Environment, Chinese Academy of Sciences, Chengdu
47 610041, China

48 ²⁴Research Institute of Soil & Fertilizer and Agricultural Water Conservation, Xinjiang Academy
49 of Agricultural Sciences, Urumqi 830091, China

50 ²⁵The Bureau of Qinghai Meteorology, Xining 810001, China

51 ²⁶Agriculture, Forestry and Water Department of Changdao County, Changdao 265800, China

52 ²⁷State Key Laboratory of Earth Surface Processes and Resource Ecology, and College of
53 Resources Science & Technology, Beijing Normal University, Beijing 100875, China

54 ²⁸Centre for Ecology & Hydrology Edinburgh, Bush Estate, Penicuik, Midlothian EH26 0QB, UK

55 ²⁹Department of Atmospheric Science, Colorado State University, Fort Collins, CO 80523, USA

56 ³⁰The Sustainable Soils and Grassland Systems Department, Rothamsted Research, Harpenden
57 AL5 2JQ, UK

58 ³¹Institute of Soil and Fertilizer, Anhui Academy of Agricultural Sciences, Hefei 230031, China

59 ³²Institute of Soil and Fertilizer, Jilin Academy of Agricultural Sciences, Changchun 130124,
60 China

61 Corresponding author: liu310@cau.edu.cn (X. J. Liu).

62

63 **Abstract:** Global reactive nitrogen (N_r) deposition to terrestrial ecosystems has
64 increased dramatically since the industrial revolution. This is especially true in recent
65 decades in China due to continuous economic growth. However, there are no
66 comprehensive reports of both measured dry and wet/bulk N_r deposition across China.
67 We therefore conducted a multiple-year study during the period mainly from 2010 to
68 2014 to monitor atmospheric concentrations of five major N_r species of gaseous NH_3 ,
69 NO_2 and HNO_3 , and inorganic nitrogen (NH_4^+ and NO_3^-) in both particles and
70 precipitation, based on a Nationwide Nitrogen Deposition Monitoring Network
71 (NNDMN, covering 43 sites) in China. Wet/bulk deposition fluxes of N_r species were
72 collected by precipitation gauge method and measured by continuous flow analyzer;
73 dry deposition fluxes were estimated using airborne concentration measurements and
74 inferential models. Our observations reveal large spatial variations of atmospheric N_r

75 concentrations and dry and wet/bulk N_r deposition. On a national basis, the annual
76 average concentrations ($1.3\text{-}47.0 \mu\text{g N m}^{-3}$) and dry plus wet/bulk deposition fluxes
77 ($2.9\text{-}83.3 \text{ kg N ha}^{-1} \text{ yr}^{-1}$) of inorganic N_r species ranked by land use as urban > rural >
78 background sites, reflecting the impact of anthropogenic N_r emission. Average dry
79 and wet/bulk N deposition fluxes were 20.6 ± 11.2 (mean \pm standard deviation) and
80 $19.3 \pm 9.2 \text{ kg N ha}^{-1} \text{ yr}^{-1}$ across China, with reduced N deposition dominating both dry
81 and wet/bulk deposition. Our results suggest atmospheric dry N deposition is equally
82 important to wet/bulk N deposition at the national scale. Therefore both deposition
83 forms should be included when considering the impacts of N deposition on
84 environment and ecosystem health.

85 **Keywords:** air pollution; reactive nitrogen; dry deposition; wet deposition; ecosystem;
86 China

87 1. Introduction

88 Humans continue to accelerate the global nitrogen (N) cycle at a record pace as rates
89 of anthropogenic reactive nitrogen (N_r) fixation have increased 20-fold over the last
90 century (Galloway et al., 2008). New N_r from anthropogenic fixation is formed
91 primarily through cultivation of N-fixing legumes, the Haber-Bosch process and
92 combustion of fossil-fuel (Galloway et al., 2013). As more N_r have been created,
93 emissions of N_r ($\text{NO}_x = \text{NO} + \text{NO}_2$, and NH_3) to the atmosphere have increased from
94 approximately 34 Tg N yr^{-1} in 1860 to 109 Tg N yr^{-1} in 2010 (Fowler et al., 2013;
95 Galloway et al., 2004); most of this emitted N_r is deposited back to land and water
96 bodies. As an essential nutrient, N supplied by atmospheric deposition is useful for all
97 life forms in the biosphere and may stimulate primary production in an ecosystem if it
98 does not exceed the ecosystem-dependent critical load (Liu et al., 2010, 2011).
99 However, long-term high levels of atmospheric N_r and its deposition can reduce
100 biological diversity (Clark et al., 2008), degrade human health (Richter et al., 2005),
101 alter soil and water chemistry (Vitousek et al., 1997) and influence the greenhouse gas
102 balance (Matson et al., 2002).

103 Nitrogen deposition occurs via dry and wet processes. Neglecting dry deposition can
104 lead to substantial underestimation of total flux as dry deposition can contribute up to
105 2/3 of total N deposition (Flechard et al., 2011; Vet et al., 2014). For quantification of
106 atmospheric deposition at the national scale, long-term monitoring networks such as
107 CAPMoN (Canada), IDAF (Africa), CASTNET/NADP (the United States), EMEP
108 (Europe) and EANET (East Asia) have been established; such networks are essential

109 for quantification of both wet and dry deposition and revealing long-term trends and
110 spatial patterns under major environmental and climate change (Skeffington and Hill,
111 2012). Wet deposition, by means of rain or snow, is relatively easily measured in
112 existing networks. In contrast, dry deposition of gases and particulate matter is much
113 more difficult to measure, and strongly influenced by factors such as surface
114 roughness, surface wetness, and climate and environmental factors (Erisman et al.,
115 2005). Direct methods (e.g., eddy correlation, chambers) and indirect methods (e.g.,
116 inferential, gradient analysis) can determine dry deposition fluxes (Seinfeld and
117 Pandis, 2006). The inferential method is widely used in many monitoring networks
118 (e.g. CASTNET and EANET), where dry deposition rates are derived from measured
119 ambient concentrations of N_r species and computed deposition velocities (Endo et al.,
120 2011; Holland et al., 2005; Pan et al., 2012). Additionally, atmospheric modeling has
121 been used as an operational tool to upscale results from sites to regions where no
122 measurements are available (Flechard et al., 2011; Zhao et al., 2015).

123 According to long-term trends observed by the above monitoring networks, N
124 deposition has decreased over the last two decades in Europe (EEA, 2011).
125 Measurements of wet deposition in the US show a strong decrease in NO_3 -N
126 deposition over most of the country (Du et al., 2014), but NH_4 -N deposition increased
127 in agricultural regions. China, as one of the most rapidly developing countries in East
128 Asia, has witnessed serious atmospheric N_r pollution since the late 1970s (Hu et al.,
129 2010; Liu et al., 2011). Accurate quantification of N deposition is key to assessing its
130 ecological impacts on terrestrial ecosystems (Liu et al., 2011). Previous modeling
131 studies (e.g., Dentener et al., 2006; Galloway et al., 2008; Vet et al., 2014) suggested
132 that central-east China was a global hotspot for N deposition. More recently, based on
133 meta-analyses of historic literature, both Liu et al. (2013) and Jia et al. (2014)
134 reported a significant increase in N wet/bulk deposition in China since the 1980s or
135 1990s. However, most measurements in China only reported wet/bulk deposition (e.g.,
136 Chen et al., 2007; Zhang et al., 2012a; Huang et al., 2013; Zhu et al., 2015) and/or dry
137 deposition (Luo et al., 2013; Shen et al., 2009; Pan et al., 2012) at a local or regional
138 scale. Although national N deposition has been investigated by Lü and Tian (2007,
139 2014), the deposition fluxes were largely underestimated due to the inclusion only of
140 gaseous NO_2 in dry deposition and not NH_3 , HNO_3 and particulate ammonium and
141 nitrate etc. Therefore, the magnitude and spatial patterns of *in situ* measured N wet
142 /bulk and dry deposition across China are still not clear.

143 Against such a background, we have established a Nationwide Nitrogen Deposition
144 Monitoring Network (NNDMN) in China in 2010, measuring both wet/bulk and dry
145 deposition. The NNDMN consists of forty-three *in-situ* monitoring sites, covering
146 urban, rural (cropland) and background (coastal, forest and grassland) areas across
147 China. The focus of the network is to conduct high-quality measurements of
148 atmospheric N_r in gases, particles and precipitation. These data provide a unique and
149 valuable quantitative description of N_r deposition in China, but have never been
150 published as a whole. The objectives of this study were therefore to: (1) obtain the
151 first quantitative information on atmospheric N_r concentrations and pollution status
152 across China; and (2) analyze overall fluxes and spatial variations of N wet/bulk and
153 dry deposition in relation to anthropogenic N_r emissions in different regions.

154 **2. Materials and Methods**

155 *2.1 Sampling sites*

156 The distribution of the forty-three monitoring sites in the NNDMN is shown in **Fig. 1**.
157 Although sampling periods varied between sites, most of our monitoring started from
158 2010 to 2014 (see Supporting Materials for details). The NNDMN comprise 10 urban
159 sites, 22 rural sites and 11 background sites (**Table S1** of the online Supplement). To
160 better analyze atmospheric N deposition results among the sites, we divided the
161 forty-three sites into six regions: north China (NC, 13 sites), northeast China (NE, 5
162 sites); northwest China (NW, 6 sites), southeast China (SE, 11 sites), southwest China
163 (SW, 6 sites), and Tibetan Plateau (TP, 2 sites), representing China's various
164 social-economical and geo-climatic regions (for details, see **Sect. A1** of the online
165 Supplement). The sites in the six regions are described using region codes (i.e., NC,
166 NE, NW, SE, SW, TP) plus site numbers such as NC1, NC2, NC3, ..., NE1, NE2, etc.
167 The longitudes and latitudes of all 43-sites ranged from 83.71 to 129.25 °E, and from
168 21.26 to 50.78 °N, respectively. Annual mean rainfall ranged from 170 to 1748 mm
169 and the annual mean air temperature ranged from -6.2 to 23.2 °C. Site names, land use
170 types and population densities are summarized in **Table S1** of the Supplement. More
171 detailed information on the monitoring sites, such as specific locations, surrounding
172 environment and possible emission sources are provided in **Sect. A2** of the
173 Supplement.

174 *2.2 Collection of gaseous and particulate N_r samples*

175 In this study ambient N_r concentrations of gaseous NH_3 , NO_2 and HNO_3 , and
176 particulate NH_4^+ (pNH_4^+) and NO_3^- (pNO_3^-) were measured monthly at the 43 sites

177 using continuous active and passive samplers. DELTA active sampling systems
178 (DEnuder for Long-Term Atmospheric sampling, described in detail in [Flechard et al.](#)
179 [\(2011\)](#) and [Sutton et al. \(2001\)](#)), were used to collect NH_3 , HNO_3 , pNH_4^+ and pNO_3^- ;
180 NO_2 samples were collected using Gradko diffusion tubes (Gradko International
181 Limited, UK) at all sampling sites. The air intakes of the DELTA system and the NO_2
182 tubes were set at a height of 2 m above the ground (at least 0.5 m higher than the
183 canopy height) at most sites. At a few sites, the DELTA systems could not be used due
184 to power constraints. Therefore, NH_3 samples were collected using ALPHA passive
185 samplers (Adapted Low-cost High Absorption, designed by the Center for Ecology
186 and Hydrology, Edinburgh, UK), while the pNH_4^+ and pNO_3^- in PM_{10} were collected
187 using particulate samplers (TSH-16 or TH-150III, Wuhan Tianhong Corp., Wuhan,
188 China). However, HNO_3 measurements were not performed due to lack of
189 corresponding passive samplers. Briefly, all the measurements of N_r concentration
190 were based on monthly sampling (one sample per month for each N_r species) except
191 at the very few sites without DELTA systems, where pNH_4^+ and pNO_3^- samples were
192 calculated from daily sampling transformed to monthly averaged data. Detailed
193 information on measuring methods, sample replication and collection are given in
194 **Sect. A3** of the Supplement with sampling periods listed in **Table S2** of the
195 Supplement. Comparisons between the ALPHA samplers and the DELTA systems at
196 six network sites for gaseous NH_3 measurements indicated that the two methods
197 provided comparable NH_3 concentrations (values between the two methods were not
198 significantly different) (cf. **Sect. A4** in the Supplement and **Fig. S1** therein).

199 *2.3 Collection of precipitation*

200 At all monitoring sites precipitation (here we define it as wet/bulk deposition which
201 contains wet and part dry deposition) samples were collected using precipitation
202 gauges (SDM6, Tianjin Weather Equipment Inc., China) located beside the DELTA
203 systems (c. 2 m). The collector, consisting of a stainless steel funnel and glass bottle
204 (vol. 2000-2500 ml), collects precipitation (rainwater, snow) without a power supply.
205 Precipitation amount was measured using a graduated cylinder (scale range: 0-10 mm;
206 division: 0.1 mm) coupled with the gauge. After each daily (8:00 am-8:00 am next
207 day) event, the collected samples were thoroughly mixed and then immediately stored
208 in clean polyethylene bottles (50 mL). All collected samples (including melted snow)
209 samples were frozen at $-18\text{ }^\circ\text{C}$ at each site until delivery to the laboratory at China
210 Agricultural University (CAU) for analysis of inorganic N (NH_4^+ and NO_3^-). The

211 gauges were cleaned with high-purity water after each collection and once every week
212 in order to avoid cross contamination.

213 *2.4 Analytical procedures*

214 In CAU's analytical laboratory, the exposed sampling trains of the DELTA systems
215 and passive samples were stored at 4 °C and analyzed at one-month intervals. The
216 HNO₃ denuders and alkaline-coated filters were extracted with 10 mL 0.05 % H₂O₂
217 in aqueous solution. The NH₃ denuders and acid-coated filters, and ALPHA samplers
218 were extracted with 10 mL high-purity water. The loaded PM₁₀ filters were extracted
219 with 50 mL high-purity water by ultrasonication for 30-60 min and then filtered
220 through a syringe filter (0.45 μm, Tengda Inc., Tianjin, China). Ammonium (NH₄⁺)
221 and nitrate (NO₃⁻) in the extracted and filtered solutions were measured with an AA3
222 continuous-flow analyzer (Bran+Luebbe GmbH, Norderstedt, Germany). The
223 detection limits were 0.01 mg N L⁻¹ for NH₄⁺ and NO₃⁻. It should be noted that
224 NO₃⁻ was converted to NO₂⁻ during the chemical analysis. So, NO₂⁻ here was included
225 in the analysis, and NO₃⁻ equals to the sum of NO₂⁻ and NO₃⁻. The disks from the
226 Gradko samplers were extracted with a solution containing sulphanilamide, H₃PO₄
227 and N-1-Naphthylethylene-diamine, and the NO₂⁻ content in the extract determined
228 using a colorimetric method by absorption at a wavelength of 542 nm. The detection
229 limit for NO₂⁻ was 0.01 mg N L⁻¹. Three laboratory and three field blank samples
230 were extracted and analyzed using the same methods as the exposed samples. After
231 correcting for the corresponding blanks, the results were used for the calculation of
232 ambient concentrations of gaseous and particulate N_r. Each collected precipitation
233 sample was filtered with a 0.45 μm syringe filter, and 15 mL filtrates frozen and
234 stored in polypropylene bottles until chemical analysis within one month. The NH₄⁺
235 and NO₃⁻ concentrations of the filtrates were determined using an AA3
236 continuous-flow analyzer as described above.

237 *2.5 Deposition flux estimation*

238 The inferential technique, which combines the measured concentration and a modeled
239 dry deposition velocity (V_d), was used to estimate the dry deposition fluxes of N_r
240 species (Schwede et al., 2011; Pan et al., 2012). The concentrations of gases (HNO₃,
241 NO₂ and NH₃) and aerosols (NH₄⁺ and NO₃⁻) were measured as described in Section
242 2.2. The monthly average V_d over China was calculated by the GEOS-Chem chemical
243 transport model (CTM) (Bey et al., 2001; <http://geos-chem.org>). The GEOS-Chem
244 CTM is driven by GEOS-5 (Goddard Earth Observing System) assimilated

245 meteorological data from the NASA Global Modeling and Assimilation Office
246 (GMAO) with a horizontal resolution of $1/2^\circ$ latitude \times $2/3^\circ$ longitude and 6-h
247 temporal resolution (3-h for surface variables and mixing depths). We used a
248 nested-grid version of GEOS-Chem for Asia that has the native $1/2^\circ \times 2/3^\circ$ resolution
249 over East Asia (70°E - 150°E , 11°S - 55°N) (Chen et al., 2009). The nested model has
250 been applied to examine atmospheric nitrogen deposition to the northwestern Pacific
251 (Zhao et al., 2015), and a similar nested model for North America has been used to
252 analyze nitrogen deposition over the United States (Zhang et al., 2012b; Ellis et al.,
253 2013). The model calculation of dry deposition of N_r species follows a standard
254 big-leaf resistance-in-series model as described by Wesely (1989) for gases and Zhang
255 et al. (2001) for aerosol. For a detailed description of the V_d calculation as well as the
256 estimation of N dry deposition, the reader is referred to the Supplement (Sect. A5),
257 with monthly and annual dry deposition velocities of N_r for different land use types
258 presented in Tables S3 and S4 therein. The model uses the land map of the Global
259 Land Cover Characteristics Data Base Version 2.0
260 (http://edc2.usgs.gov/glcc/globdoc2_0.php), which defines the land types (e.g., urban,
261 forest, etc.) at the native $1 \text{ km} \times 1 \text{ km}$ resolution and is then binned to the model
262 resolution as fraction of the grid cell covered by each land type. The model $1/2^\circ$
263 resolution may coarsely represent the local land characteristics at the monitoring sites.
264 Future work using a single-point dry deposition model as for CASTNET (Clarke et al.,
265 1997) would further improve the dry deposition flux estimates, but that requires
266 concurrent *in-situ* measurements of meteorological variables which are not available
267 at present.

268 Wet/bulk N deposition flux was calculated as the product of the precipitation amount
269 and the concentration of N_r species in precipitation, using the following equations (1)
270 and (2):

$$271 \quad C_w = \sum_{i=1}^n (C_i P_i) / \sum_{i=1}^n P_i \quad (1)$$

272 where C_w is the volume-weighted mean (VWM) concentration (mg N L^{-1}) calculated
273 from the n precipitation samples within a month or a year, and the individual sample
274 concentration C_i is weighted by the rainfall amount P_i for each sample.

$$275 \quad D_w = P_t C_w / 100 \quad (2)$$

276 where D_w is the wet/bulk deposition flux (kg N ha^{-1}), P_t is the total amount of all
277 precipitation events (mm), and 100 is a unit conversion factor.

278 2.6 Statistics

279 A one-way analysis of variance (ANOVA) and nonparametric t-tests were conducted
280 to examine the differences in the investigated variables between sites (urban, rural and
281 background) and between the six regions. Linear regression analysis was used to
282 analyze the relationships among annual wet N deposition flux, annual precipitation
283 amount and annual VWM concentration of inorganic N in precipitation. All analyses
284 were performed using SPSS 11.5 (SPSS Inc., Chicago, IL, USA). Statistically
285 significant differences were set at P values < 0.05 .

286 **3. Results**

287 *3.1 Concentrations of N_r species in air*

288 Monthly mean concentrations of NH_3 , NO_2 , HNO_3 , pNH_4^+ and pNO_3^- were
289 0.08-34.8, 0.13-33.4, 0.02-4.90, 0.02-55.0 and 0.02-32.1 $\mu\text{g N m}^{-3}$, respectively (**Fig.**
290 **S2a-e**, Supplement). The annual mean concentrations of gaseous and particulate N_r
291 were calculated for each site from the monthly N_r concentrations (**Fig. 2a**), and
292 further were averaged for land use types in the six regions (**Fig. 3a-e**) and the whole
293 nation (**Fig. 4a**) according to geographical location and the classification of each site.
294 Annual mean NH_3 concentrations ranged from 0.3 to 13.1 $\mu\text{g N m}^{-3}$, with an overall
295 average value of 6.1 $\mu\text{g N m}^{-3}$. In NC, SE and SW, the NH_3 concentrations at the
296 urban sites (average for the three regions, $9.5 \pm 2.1 \mu\text{g N m}^{-3}$) were about 1/3 higher
297 than at the rural sites ($6.2 \pm 2.3 \mu\text{g N m}^{-3}$) and were almost twice of those at the
298 background sites ($4.8 \pm 1.4 \mu\text{g N m}^{-3}$), whereas in NE and NW NH_3 concentrations
299 were lower at the urban sites (average two regions, $5.5 \pm 3.2 \mu\text{g N m}^{-3}$) than at the
300 rural sites ($8.8 \pm 0.3 \mu\text{g N m}^{-3}$) but 4.6-times greater than at the background sites (1.2
301 $\pm 0.5 \mu\text{g N m}^{-3}$). Comparing land use types by region, annual NH_3 concentrations at
302 the rural sites in northern regions (NC, NE and NW) were approximately equal, which
303 on average were 1.8-times greater than the average of southern rural sites. In contrast,
304 annual NH_3 concentrations at urban and background sites ranked in the order: SW >
305 NC > NW > SE > TP > NE, and SW > NC > SE > NW > TP > NE, respectively (**Fig.**
306 **3a**). Annual mean NO_2 concentrations showed similar spatial variations (0.4 to 16.2
307 $\mu\text{g N m}^{-3}$) to those of NH_3 , and overall averaged 6.8 $\mu\text{g N m}^{-3}$. In the six regions, the
308 NO_2 concentrations at urban sites were 1.4-4.5 times higher than those at rural sites,
309 and were even 2.0-16.6 times higher than the background sites (except for SW). By
310 comparison among regions, annual mean NO_2 concentrations at rural sites in NC were
311 about 2.6-times higher than in NE and NW, and overall averaged NO_2 concentrations

312 in northern rural China (NC, NE and NW, $5.7 \pm 3.5 \mu\text{g N m}^{-3}$) were comparable to
313 those at southern rural sites (average of SE and SW, $5.1 \pm 0.1 \mu\text{g N m}^{-3}$). As for urban
314 and background sites, the annual mean NO_2 concentrations followed the order: NC >
315 NW > SE > SW > NE > TP, and SW > NC > SE > NE > NW > TP, respectively (**Fig.**
316 **3b**). Annual mean HNO_3 concentrations were relatively low everywhere (from 0.1 to
317 $2.9 \mu\text{g N m}^{-3}$, averaging $1.3 \mu\text{g N m}^{-3}$). In all regions except NE and TP, the HNO_3
318 concentrations were highest at the urban sites (averages: $1.7\text{-}2.4 \mu\text{g N m}^{-3}$), followed
319 by the rural sites ($0.8\text{-}1.6 \mu\text{g N m}^{-3}$), and were lowest at the background sites ($0.2\text{-}1.1$
320 $\mu\text{g N m}^{-3}$). The HNO_3 concentrations were comparable for the same land use types
321 across northern and southern monitoring sites, on average, 1.8 vs. 1.8, 1.2 vs. 1.0, and
322 0.6 vs. $0.8 \mu\text{g N m}^{-3}$ at the urban, rural and background sites, respectively (**Fig. 3c**).
323 The annual mean concentrations of pNH_4^+ and pNO_3^- were in the ranges of $0.2\text{-}18.0$
324 $\mu\text{g N m}^{-3}$ (average $5.7 \mu\text{g N m}^{-3}$) and $0.2\text{-}7.7 \mu\text{g N m}^{-3}$ (average $2.7 \mu\text{g N m}^{-3}$),
325 respectively. Annual pNH_4^+ concentrations show a decreasing trend of urban > rural >
326 background in all regions (except NE), where relatively higher concentrations were
327 observed at the rural sites than the urban sites, and in SE, where no clear difference
328 were observed among three land use types (**Fig. 3d**). In contrast, annual
329 pNO_3^- concentrations showed a declining trend of urban > rural > background in all
330 regions (**Fig. 3e**). Overall, annual mean concentrations of both pNH_4^+ and pNO_3^- at
331 all land use types were both slightly higher in northern China (NC, NE and NW) than
332 in southern China (SE, SW and TP).

333 In total, annual mean concentrations of gaseous and particulate N_r in air were $1.3\text{-}47.0$
334 $\mu\text{g N m}^{-3}$ among all sampling sites. The total annual concentrations of measured N_r
335 generally decreased in the order of urban > rural > background in all regions except
336 NE (**Fig. 3f**).

337 *3.2 Concentrations of N_r species in precipitation*

338 The monthly VWM concentrations of inorganic N_r species at the forty-three sampling
339 sites during the study period ranged from 0.01 to 27.1 mg N L^{-1} for $\text{NH}_4^+\text{-N}$ and from
340 0.02 to 27.9 mg N L^{-1} for $\text{NO}_3^-\text{-N}$ (**Fig. S3**, Supplement). The annual VWM
341 concentrations of $\text{NH}_4^+\text{-N}$ and $\text{NO}_3^-\text{-N}$ across all sites were in the ranges of $0.2\text{-}4.3$
342 and $0.1\text{-}2.5 \text{ mg N L}^{-1}$, respectively, with averages of 1.6 and 1.3 mg N L^{-1} (**Fig. 2b**).
343 The urban-rural-background distributions of annual VWM concentrations of $\text{NH}_4^+\text{-N}$
344 and $\text{NO}_3^-\text{-N}$ were, respectively, fairly coincided with corresponding reduced (i.e. NH_3
345 and pNH_4^+) and oxidized N_r (i.e. HNO_3 and pNO_3^-) in all regions except $\text{NH}_4^+\text{-N}$ in

346 SE and NO_3^- -N in NW (**Figs. 3g and h**). Conversely, the regional variations in annual
347 VWM concentrations of NH_4^+ -N and NO_3^- -N for the three land use types were not
348 consistent with corresponding reduced and oxidized N_r , respectively. On a national
349 basis, the VWM concentrations of NH_4^+ -N and NO_3^- -N were both decreased in the
350 order urban \geq rural $>$ background (**Fig. 4b**). The annual total inorganic N (TIN)
351 concentrations in precipitation across all sites were 0.4-6.0 mg N L⁻¹, decreasing from
352 urban to background sites in all regions (except NE) as well as on a national basis
353 (**Figs. 3i and 4b**).

354 3.3 Dry deposition of N_r species

355 The annual dry deposition fluxes of NH_3 , NO_2 , HNO_3 , pNH_4^+ and pNO_3^- were in the
356 ranges of 0.5-16.0, 0.2-9.8, 0.2-16.6, 0.1-11.7 and 0.1-4.5 kg N ha⁻¹ yr⁻¹, and averaged
357 8.2, 3.2, 5.4, 3.2 and 1.5 kg N ha⁻¹ yr⁻¹, respectively (**Fig. 5a**). The total dry N
358 deposition across all sites ranged from 1.1 to 52.2 kg N ha⁻¹ yr⁻¹ (averaged 20.6 ± 11.2
359 kg N ha⁻¹ yr⁻¹). Gaseous N species were the primary contributors to total
360 dry-deposited N, ranging from 60% to 96%, despite of the missing HNO_3 data at a
361 few sites. In general, NH_3 was predominant N_r species in total dry N deposition and
362 accounted for 24-72%, compared with 1-43% from NO_2 and 9-37% from HNO_3 .
363 Comparing land use types in each region, spatial pattern of individual fluxes is fairly
364 consistent with that of their respective concentrations except that of NH_3 for NC, that
365 of NO_2 for SW, those of NO_2 and pNH_4^+ for NW and those of almost all measured N_r
366 species for NE (**Figs. 3a-e and 6a-e**). Furthermore, a consistent picture is also seen
367 for the total flux (sum of fluxes of five N_r species) at each land use type (**Figs. 5f and**
368 **6f**). Among the six regions, regional variations of individual fluxes at each land use
369 type generally differed from those of their respective concentrations. Similarly, the
370 inconsistent behavior appeared for the total fluxes at urban and rural sites but not at
371 background site. On a national basis, there was no significant difference ($p > 0.05$) in
372 the total dry N deposition fluxes between urban (26.9 kg N ha⁻¹ yr⁻¹) and rural (23.0
373 kg N ha⁻¹ yr⁻¹) sites, both of which were significantly higher than background site
374 (10.1 kg N ha⁻¹ yr⁻¹). Also, a similar pattern was found for the dry deposition flux of
375 each N_r species among different land use types (**Fig. 4c**).

376 3.4 Wet/bulk deposition of N_r species

377 Annual wet/bulk N deposition fluxes at the forty-three sites ranged from 1.0 to 19.1
378 kg N ha⁻¹ yr⁻¹ for NH_4^+ -N and from 0.5 to 20.1 kg N ha⁻¹ yr⁻¹ for NO_3^- -N (**Fig. 5b**).

379 The annual wet/bulk deposition fluxes of NH_4^+ -N were, on average, 1.3 times those
380 of NO_3^- -N. The total annual wet/bulk N (NH_4^+ -N+ NO_3^- -N) deposition fluxes across
381 all the sites were 1.5-32.5 kg N ha⁻¹ yr⁻¹ (average 19.3 kg N ha⁻¹ yr⁻¹), with a large
382 spatial variation. Region variation of annual wet N deposition followed the order of
383 NC > SE > SW > NE > NW > TP for NH_4^+ -N, and SE > NC > SW > NE > TP > NW
384 for NO_3^- -N, both of which differed from their orders of annual VWM concentration,
385 reflecting differences in annual precipitation amount. Annual total wet/bulk N
386 deposition fluxes averaged 24.6, 13.6, 7.4, 24.4, 17.6 and 7.6 kg N ha⁻¹ yr⁻¹,
387 respectively, in NC, NE, NW, SE, SW and TP (**Fig. 5b**). At national scale, annual
388 wet/bulk deposition fluxes of total inorganic N and/or each N_r species at urban and
389 rural sites were comparable but significantly higher ($p < 0.05$) than those at
390 background sites (**Fig. 4d**).

391 3.5 Total annual dry and wet deposition of N_r species

392 The total (dry plus wet/bulk) annual N deposition at the 43 sites ranged from 2.9 to
393 83.3 kg N ha⁻¹ yr⁻¹ (average 39.9 kg N ha⁻¹ yr⁻¹) for the period, with 23-83%
394 dry-deposited (**Fig. 5c**). Separated by land use types, total annual mean N deposition
395 fluxes were 49.7, 44.3 and 26.0 kg N ha⁻¹ at the urban, rural and background sites,
396 respectively, reflecting different anthropogenic impacts. In our network, the NH_x (i.e.
397 wet/bulk NH_4^+ -N deposition plus dry deposition of NH_3 and particulate NH_4^+)/ NO_y
398 (wet/bulk NO_3^- -N deposition plus dry deposition of NO_2 , HNO_3 and particulate NO_3^-)
399 ratio at urban sites (from 0.8 to 1.8, averaging 1.2) was not significantly different
400 ($p > 0.05$) from rural (from 0.5 to 2.7, averaging 1.3) and background (from 1.0 to 2.5,
401 averaging 1.6) sites. On a regional basis, the relative importance of dry vs. wet/bulk N
402 deposition to the total deposition were different in the six regions, 57% vs. 43% in NC,
403 54% vs. 46% in NE, 61% vs. 39% in NW, 42% vs. 58% in SE, 55% vs. 45% in SW,
404 and 50% vs. 50% in TP (**Fig. 7**).

405 4. Discussion

406 4.1 Concentration of N_r species in air and precipitation

407 China is facing serious atmospheric N_r pollution induced by anthropogenic N_r
408 emissions (Liu et al., 2011, 2013). The present study shows that monthly N_r
409 concentrations of species, through comparisons among regions, have a distinct spatial
410 variability with values significantly higher (all $p < 0.05$) in NC and significantly lower
411 (all $p < 0.05$) in TP. Annual mean NH_3 and NO_2 concentrations at most sampling sites
412 are in good agreement with the emission inventory and satellite observations by Gu et

413 [al. \(2012\)](#), who reported NH₃ hotspots in the North China Plain and South Central
414 China such as Jiangsu and Guangdong provinces, while NO_x hotspots were mainly in
415 more developed regions such as the Jing-Jin-Ji (Beijing-Tianjin-Hebei), the Yangtze
416 River Delta and the Pearl River Delta. Our results confirm that NC, which consumes
417 large quantities of fertilizers (for food production) and fossil fuel (for energy supply)
418 ([Zhang et al., 2010](#)) experiences the most serious N_r pollution in China; TP is the least
419 polluted region due to much less human activity. When considering different land use
420 types, the average total annual N_r concentrations ranked urban > rural > background,
421 with significant differences (all $p < 0.05$) among them, despite site-to-site variability
422 within regions. This reflects the dominant role of human activity on atmospheric N_r.
423 For individual N_r species, higher mean concentrations were observed at the urban
424 sites than at rural and background sites (**Fig. 4a**). Higher NH₃ concentration in urban
425 areas may be associated with NH₃ emissions from biological sources, such as human,
426 sewage disposal systems and refuse containers ([Reche et al., 2002](#)). In addition, NH₃
427 can be produced by over-reduction of NO in automobile catalytic converters ([Behera
428 et al., 2013](#)), increasing ambient NH₃ concentrations in urban areas with high traffic
429 densities. Between 2006 and 2013, the number of civil vehicles increased from 2.39 to
430 5.17 million in Beijing and from 0.46 to 1.72 million in Zhengzhou ([CSY, 2007-2014](#)),
431 which is likely to have resulted in elevated NH₃ emissions. Higher NO₂
432 concentrations are expected in urban areas due to NO_x emissions from the combustion
433 of fossil fuels ([Li and Lin, 2000](#)), and also lead to higher HNO₃ concentrations in
434 urban areas via NO₂ oxidation.

435 The higher pNH₄⁺ and pNO₃⁻ concentrations observed at urban sites mainly resulted
436 from the high concentrations at the northern urban sites (NC1~3, NW1 and NW2)
437 (**Fig. 2a and Fig. S2d, e** in Supplement). This is probably due to the fact that cities in
438 northern China, such as Beijing and Zhengzhou in NC and Urumqi in NW, are being
439 surrounded by intensive agricultural production. Rapid developments along with
440 urbanization in suburban areas shorten the transport distance between NH₃ emitted
441 from agriculture and SO₂ and NO_x emitted from fossil fuel combustion ([Gu et al.,
442 2014](#)). This allows the pollutants to react more readily and form aerosols (e.g. PM_{2.5}),
443 leading to high concentrations of pNH₄⁺ and pNO₃⁻ near or within cities. This
444 explanation is supported by the recent [MEPC \(2013\)](#) report that the annual average
445 PM_{2.5} concentrations in the cities of Beijing, Zhengzhou and Urumqi were more than
446 twice the Chinese annual mean PM_{2.5} standard value of 35 μg m⁻³, whereas cities such

447 as Guangzhou and Xining with little surrounding agricultural production had lower
448 PM_{2.5} concentrations. In China's 12th Five Year Plan (2011–2015), nationwide
449 controls on NO_x emissions will be implemented along with controls on SO₂ and
450 primary particle emissions (Wang et al., 2014). In order to better improve the regional
451 air quality for metropolitan areas; our results suggest that strict control measures on
452 both NH₃ and NO_x would be beneficial in NC, at least in the suburban areas.

453 Rural sites in this study also had relatively high concentrations of all measured N_r
454 species in air, altogether ranking in the order of NC > NE > NW > SE > SW (Fig. 3f).
455 The higher concentrations in northern China are mainly due to the combined effect of
456 high NH₃ emissions from N fertilized farmland (Zhang et al., 2008a) and urban air
457 pollution (e.g. NO₂, HNO₃, pNH₄⁺ and pNO₃⁻) transported from population centers to
458 the surrounding rural areas (Luo et al., 2013). The lower air concentrations of N_r
459 species at background sites can be ascribed to the lack of both substantial agricultural
460 and industrial emissions. Additionally, higher wind speeds occurred at some
461 background areas (e.g. NC12, NC13 and NW4) (Table S1, Supplement), favoring the
462 dispersion of atmospheric pollutants.

463 We found that regional variations in N_r concentrations in precipitation were not fully
464 in accordance with ambient N_r concentrations (see Sect. 3.2) when assessed by land
465 use types. It is commonly accepted that N concentrations in precipitation are affected
466 by the amount of precipitation (Yu et al., 2011). Negative correlations between
467 precipitation amount and monthly volume-weighted concentrations of NH₄⁺-N and
468 NO₃⁻-N were obtained by fitting exponential models in all six regions (Fig. S4,
469 Supplement), indicating a dilution effect of rainwater on inorganic N concentration.
470 The relationships were not significant ($p > 0.05$) in NW and TP, which is probably
471 caused by low precipitation amounts at or near the sampling sites (Fig. S5,
472 Supplement). Nevertheless, dilution could explain some of the regional differences in
473 precipitation N concentrations.

474 4.2 Dry and wet/bulk deposition of N_r species

475 A significant ($p < 0.001$) positive correlation was observed between annual dry N
476 deposition and total annual concentrations of atmospheric N_r species across all sites
477 (Fig. S6, Supplement). Therefore, higher concentrations of N_r species at urban sites
478 led to higher dry deposition rates compared with rural and background sites, mainly
479 attributable to elevated N_r emissions from urban sources (e.g., non-agricultural NH₃
480 emissions from landfills, wastewater treatments and NO_x emissions from traffic

481 vehicles and power plants) and rapid development of intensive agricultural production
482 in suburban areas surrounding cities; regardless of differences in dry deposition
483 velocities of various N_r species in different land use types. At the national scale, dry N
484 deposition rates contributed almost half (23-83%, averaging 52%) of the total
485 inorganic N deposition, indicating the importance of dry deposition monitoring for
486 comprehensive N deposition quantification.

487 In this study, regional variations of annual wet/bulk N deposition fluxes of NH_4^+ -N,
488 NO_3^- -N and their sum showed different spatial patterns to those of corresponding
489 annual VWM concentrations of them in precipitation (see Sect. 3.4). These findings,
490 together with no significant differences ($p>0.05$) in total annual wet/bulk N deposition
491 between NC and SE, reflect, not surprisingly, that regional wet/bulk N deposition is
492 dependent not only on N_r concentrations in precipitation but also on annual rainfall
493 amounts. As shown in Fig. 8, annual wet/bulk deposition fluxes of NH_4^+ -N and
494 NO_3^- -N both showed significantly positive correlations with the corresponding annual
495 VWM concentrations of inorganic N and annual precipitation amount, especially for
496 NH_4^+ -N, that more significant was found for precipitation amount than concentration.
497 The measured wet/bulk N deposition rates (average $19.3 \text{ kg N ha}^{-1} \text{ yr}^{-1}$) were almost
498 twice the earlier average wet deposition value of $9.9 \text{ kg N ha}^{-1} \text{ yr}^{-1}$ for period of
499 1990-2003 in China (Lü and Tian, 2007). Our results show similar regional patterns
500 and comparable magnitudes to those measured in the 2000s in China as reported by
501 Jia et al. (2014) ($\sim 14 \text{ kg N ha}^{-1} \text{ yr}^{-1}$, wet deposition) and Liu et al. (2013) ($\sim 21 \text{ kg N}$
502 $\text{ha}^{-1} \text{ yr}^{-1}$, bulk deposition).

503 The NH_4^+ -N/ NO_3^- -N ratio in wet/bulk deposition can be used to indicate the relative
504 contribution of N_r from agricultural and industrial activities to N deposition (Pan et al.,
505 2012; Zhan et al., 2015; Zhu et al., 2015) because the major anthropogenic source of
506 NH_4^+ -N in precipitation is NH_3 volatilized from animal excrement and the application
507 of nitrogenous fertilizers in agriculture, while anthropogenic sources of NO_3^- -N in
508 precipitation originate from NO_x emitted from fossil fuel combustion in transportation,
509 power plant and factories (Cui et al., 2014). In this study the overall annual average
510 ratio of NH_4^+ -N/ NO_3^- -N in wet/bulk deposition was 1.3 ± 0.5 (standard deviation),
511 with an increasing (but not significant) trend for urban (1.2 ± 0.6), rural (1.3 ± 0.4),
512 and background (1.5 ± 0.4) sites (Fig. 5b). Our measured ratio was slightly lower than
513 average values of 1.6 in Europe (Holland et al., 2005) and 1.5 in the United States (Du
514 et al., 2014), and similar to an average value (1.2) reported elsewhere for 2013 in

515 China (Zhu et al., 2015). Based on these findings, we conclude that NH_4^+ -N from
516 agricultural sources still dominates wet/bulk N deposition but the contribution has
517 decreased drastically between the 1980s and the 2000s (Liu et al., 2013). Reduced N
518 also contributed more than oxidized N to the total N deposition, and the ratio of
519 reduced to oxidized N deposition overall averaged 1.6 ± 0.7 in dry deposition and 1.4
520 ± 0.4 in the total deposition (Fig. 5a, c).

521 The overall mean annual deposition fluxes (wet/bulk plus dry) of NH_x and NO_y for
522 the period 2010-2014 was graded into five levels and plotted on maps showing the
523 spatial distribution of NH_3 and NO_x emissions (Fig. 9a, b). The anthropogenic
524 emission data of NH_3 and NO_x for the year 2010 in China were obtained from
525 the GAINS (Greenhouse Gas and Air Pollution Interactions and Synergies) model
526 (<http://www.iiasa.ac.at/>), and emission details for the 33 provinces of China are
527 summarized in Table S5 of the Supplement. The spatial patterns of estimated NH_x
528 and NO_y deposition compare reasonably well with the regional patterns of NH_3 and
529 NO_x emissions, respectively, even though the emission data were estimated at the
530 province scale. With emission data, N deposition can be used to distinguish regional
531 differences in reactive N_r pollution. Across six regions, significantly positive
532 correlations were found between NH_3 emissions and NH_x deposition fluxes
533 ($R^2=0.888$, $p<0.01$) (Fig. 9c), and between NO_x emissions and NO_y deposition fluxes
534 ($R^2=0.805$, $p<0.05$) (Fig. 9d), implying that the N deposition fluxes to the six regions
535 are strongly dependent on the spatial pattern of anthropogenic N_r emissions among
536 the regions. The slopes of the relationships of NH_x vs NH_3 , and NO_y vs NO_x were
537 0.51 and 0.48, which could be roughly interpreted that NH_x and NO_y deposition
538 fluxes represent about 51% NH_3 and 48% NO_x emissions, respectively.

539 For all Chinese regions except NC we cannot compare our data with other studies
540 because observations for different pollution climate sites in other regions are lacking.
541 For NC, the overall average total N deposition was $56.2 \pm 14.8 \text{ kg N ha}^{-1} \text{ yr}^{-1}$, 13-32%
542 lower than the previously estimated values in Northern China (Pan et al., 2012; Luo et
543 al., 2013). This difference may reflect differences in the numbers of sampling sites,
544 land use type and assumed dry deposition velocities. As expected, our estimated
545 deposition was substantially higher than the results of Lü and Tian (2007), who
546 suggested that the total N deposition ranged from 13 to 20 $\text{kg N ha}^{-1} \text{ yr}^{-1}$ in NC. This
547 is attributed to their omission of many major species (e.g., gaseous NH_3 , HNO_3 and
548 particulate N_r) from their data.

549 Compared to dry and wet N deposition fluxes estimated by CASTNET in the United
550 States, EMEP in Europe, and EANET sites in Japan, the average values of dry and
551 wet/bulk deposition in China are much higher (**Table 1**). In addition, on the basis of
552 2001 ensemble-mean modeling results from 21 global chemical transport models ([Vet
553 et al., 2014](#)), three regions of the globe where total deposition is very high: western
554 Europe (with levels from 20.0 to 28.1 kg N ha⁻¹ yr⁻¹); South Asia (Pakistan, India and
555 Bangladesh) from 20.0 to 30.6 kg N ha⁻¹ yr⁻¹ and East Asia from 20 to 38.6 kg N
556 ha⁻¹ yr⁻¹ in eastern China (the global maximum). Extensive areas of high deposition
557 from 10 to 20 kg N ha⁻¹ yr⁻¹ appear in the eastern U.S. and southeastern Canada as
558 well as most of central Europe. Small areas with total deposition of N from 10 to 20
559 kg N ha⁻¹ yr⁻¹ are present, and very large areas of the continents have deposition from
560 2 to 10 kg N ha⁻¹ yr⁻¹. In contrast, the present study shows much higher total
561 deposition flux (39.9 kg N ha⁻¹ yr⁻¹) at a national scale. In China, the consumption
562 rates of chemical fertilizer and fossil fuel have increased 2.0- and 3.2-fold,
563 respectively, between the 1980s and the 2000s ([Liu et al., 2013](#)). As a result, the
564 estimated total emission of NH₃ reached 9.8 Tg in 2006, contributing approximately
565 15% and 35% to the global and Asian NH₃ emissions ([Huang et al., 2012](#)), and NO_x
566 emissions from fossil fuel combustion increased from 1.1 Tg N in 1980 to about 6.0
567 Tg N in 2010 ([Liu et al., 2013](#)). The increasing NO_x and NH₃ emissions in China led
568 to higher atmospheric N deposition than those observed in other regions.

569 According to [Endo et al. \(2011\)](#), the low dry deposition fluxes in CASTNET, EMEP
570 and Japan's EANET network are due at least partly to low concentrations of N_r
571 compounds and/or the omission of dry deposition fluxes of major N_r species (e.g.,
572 NO₂ and NH₃) from the data. Meanwhile, the low wet deposition fluxes at these
573 networks are likely to be a result of the combined effects of low amounts of
574 precipitation and, especially, low atmospheric N_r concentrations. In addition,
575 emissions of nitrogen compounds in other parts of the world are declining. In the U.S.,
576 for example, NO_x emissions from the power sector and mobile sources were reduced
577 by half from 1990 to 2010 ([Xing et al., 2013](#)), which explained the declined N
578 deposition fluxes during period of 1990-2009 observed at 34 paired dry and wet
579 monitoring sites in the eastern US ([Sickles II et al., 2015](#)). In Europe, the total NO_x
580 and NH₃ emissions decreased by 31% and 29% from 1990 to 2009 ([Torseth et al.,
581 2012](#)). N deposition has decreased or stabilized in the United States and Europe since
582 the late 1980s or early 1990s with the implementation of stricter legislation to reduce

583 emissions (Goulding et al., 1998; Holland et al., 2005). However, wet deposition of
584 ammonia, which is not regulated, has increased in recent years in the U.S. (Du et al.,
585 2014).

586 *4.3 Implications of monitoring N_r concentration and deposition on regional N* 587 *deposition simulation*

588 Our results show that atmospheric concentrations and deposition of N_r in China were
589 high in the 2000s, although the government has made considerable efforts to control
590 environmental pollution by improving air quality in mega cities during and after the
591 2008 Beijing Summer Olympic Games (Wang et al., 2010; Chan and Yao, 2008).
592 Ideally, the spatial distribution of monitoring sites should reflect the gradients in the
593 concentrations and deposition fluxes of atmospheric N_r species. Given the fact that the
594 arithmetic averages used in this study cannot give a completely accurate evaluation of
595 N_r levels for the regions of China due to the limited numbers of monitoring sites and
596 ecosystem types, it is important to develop and improve the quantitative methods for
597 determining N deposition across China.

598 Numerical models are very useful tools to quantify atmospheric N deposition
599 (including both spatial and temporal variations), but a challenge to the modeling
600 approaches is that observations to validate the simulated concentrations and
601 deposition fluxes are often lacking. In our study 43 monitoring sites were selected in a
602 range of ecosystem types to provide more representative regional information on
603 atmospheric N deposition in China. Although those measurements cannot define all
604 aspects of N deposition across different regions, they add substantially to existing
605 knowledge concerning the spatial patterns and magnitudes of atmospheric N
606 deposition. The present measurements will be useful for better constraining emission
607 inventories and evaluating simulations from atmospheric chemistry models. In future
608 studies we will use models (e.g., FRAME, Dore et al., 2012) integrated with
609 measurements from our monitoring network to fully address the spatial-temporal
610 variations of atmospheric N deposition and its impacts on natural and semi-natural
611 ecosystems at the regional/national level.

612 *4.4 Uncertainty analysis of the N dry and wet deposition fluxes*

613 The dry deposition fluxes were estimated by combining measured concentrations with
614 modeled V_d . As summarized in **Table S4**, our estimates of dry deposition velocities
615 for different N_r species are generally consistent with the estimates in previous studies
616 (e.g., Flechard et al., 2011; Pan et al., 2012). Some uncertainties may still exist in the

617 inputs for dry deposition modeling. For example, underlying surface parameters (e.g.,
618 surface roughness length and land type) strongly affect dry deposition through their
619 effect on both deposition velocity and the absorbability of the ground surface to each
620 of the gaseous and particulate N_r species (Loubet et al., 2008). In addition, there is
621 uncertainty in the deposition fluxes for both pNH_4^+ and pNO_3^- in our network,
622 resulting from the difference between the cut-off sizes of particles in the samplers and
623 that defined in the modeled V_d which were calculated for atmospheric $PM_{2.5}$ in
624 GEOS-Chem model. For example, the cut-off sizes of the samples can collect also
625 coarse NO_3^- particles (e.g. calcium nitrate) but should have little effect on NH_4^+
626 particles (mainly in the fine scale $<1\mu m$) (Tang et al., 2009), resulting in an
627 underestimation of pNO_3^- deposition. Furthermore, NH_3 fluxes over vegetated land
628 are bi-directional and the net direction of this flux is often uncertain. A so-called
629 canopy compensation point was used in previous studies (Sutton et al., 1998) to
630 determine the direction of the NH_3 flux. Since the principle of bi-directional NH_3
631 exchange was not considered in this study, NH_3 deposition may be overestimated at
632 rural sites with relatively high canopy compensation points (e.g. up to $5 \mu g N m^{-3}$) due
633 to fertilized croplands or vegetation (Sutton et al., 1993). On the other hand, the total
634 dry deposition flux in this study may be underestimated due to omission of the
635 dry-deposited organic N species in our network and missing HNO_3 data at very few
636 sites as noted earlier (see Sect. 2.2). The organic N species have been found as
637 important contributors to the N dry deposition. For example, PAN accounted for 20%
638 of the daytime, summertime NO_y ($NO + NO_2 + HNO_3 + NO_3^- + PAN$) dry deposition
639 at a coniferous forest site (Turnipseed et al., 2006). However, the contribution of PAN
640 and other known atmospheric organic nitrates to total N_r inputs must be minor on the
641 annual time scale, as reported by Flechard et al. (2012). In previous work, dry
642 deposition flux was inferred from atmospheric N_r concentrations and a
643 literature-based annual mean deposition velocity (Shen et al., 2009), or reported by
644 Luo et al. (2013) who did not consider the different dry deposition velocities of
645 various N_r species among different land use types. Clearly, in this study we have
646 greatly improved the estimation of dry deposition, but further work is still required to
647 increase the reliability and accuracy of N dry deposition values.

648 Since wet/bulk deposition was measured directly, the reported fluxes are considered
649 more accurate than dry deposition fluxes but still some uncertainties exist. On one
650 hand, the estimated fluxes obtained from the open precipitation samplers contain

651 contributions from wet plus unquantifiable dry deposition (including both gases and
652 particles) and therefore likely overestimate actual wet deposition (Cape et al., 2009).
653 For example, our previous research showed that annual unquantifiable dry deposition
654 (the difference between bulk and wet deposition, approx. 6 kg N ha⁻¹ on average)
655 accounted for 20% of bulk N deposition based on observations at three rural sites on
656 the North China Plain (Zhang et al., 2008b). This contribution increased to 39% in
657 urban areas based on a recent measurement (Zhang et al., 2015). On the other hand,
658 dissolved organic N compounds, which have been observed to contribute to be around
659 25-30% of the total dissolved nitrogen in wet deposition around the world (Jickells et
660 al., 2013) and approximately 28% of the total atmosphere bulk N deposition in China
661 (Zhang et al., 2012b), were not considered in the present study. Their exclusion here
662 would contribute to an underestimation of the total wet N deposition.

663 Although the NNDMN is the only long-term national deposition network to monitor
664 both N wet/bulk and dry deposition in China till now, large areas of the country or
665 islands lack of sampling points may be missing hotspots or pristine sites of N
666 deposition. The implementation of an adequate monitoring program is also difficult at
667 present in some regions (e.g., northwest China and Tibetan Plateau). To address this
668 issue, more new monitoring sites, covering regions with both extremely low and high
669 N_r emissions, should be set up in the NNDMN in future work.

670 **Conclusions**

671 Our study represents the first effort to investigate inorganic dry and wet/bulk N
672 deposition simultaneously, based on a nationwide monitoring network in China. We
673 consider this unique dataset important not only for informing policy-makers about the
674 abatement of pollutant emissions and ecosystem protection but also to validate model
675 estimations of N deposition at the regional/national scale in China. The major results
676 and conclusions are as follows.

- 677 1. Distinct spatial variability in annual mean concentrations of N_r species in air and
678 precipitation was observed, with different regional variations based on land use
679 type across the six regions. On a national basis, the order of total concentrations of
680 N_r species, as well as each species, was urban > rural > background.
- 681 2. Large spatial variations were observed for both dry and wet/bulk N deposition. The
682 spatial patterns of dry and wet/bulk deposition both followed urban > rural >

683 background at the national scale. Dry N deposition correlated well with total
684 concentrations of N_r in the air, but differences were found between patterns of
685 wet/bulk N deposition and the N_r concentration in precipitation. This reflects the
686 combining effect of both N_r concentrations and precipitation amounts on regional
687 wet/bulk N deposition.

688 3. Spatial distribution of total annual N deposition fluxes across all sites compared
689 well with the spatial pattern of nitrogen emissions at the regional level. When
690 considering land use type, the total N deposition was highest at urban sites,
691 followed by rural sites and background sites, mainly attributable to N_r emissions
692 from urban sources and rapid development of intensive agricultural production in
693 suburban areas.

694 4. Dry deposition fluxes of N_r species on average contributed 52% of the total N
695 deposition ($39.9 \text{ kg N ha}^{-1} \text{ yr}^{-1}$) across all sites, indicating the importance of dry
696 deposition monitoring for a complete N deposition assessment at the national
697 scale.

698 5. Annual average ratios of reduced N/oxidized N in dry and wet/bulk deposition
699 were respectively 1.6 and 1.3, and 1.4 for the total deposition. It shows that
700 reduced N, mainly from agricultural sources, still dominates dry, wet/bulk, and
701 total N deposition in China.

702

703 **Acknowledgments**

704 This study was supported by the Chinese National Basic Research Program
705 (2014CB954202), the China Funds for Distinguished Young Scholars of NSFC
706 (40425007), and the National Natural Science Foundation of China (31121062,
707 41321064 and 41405144). The authors thank all technicians at monitoring sites in
708 NNDMN.

709

710 **References**

711 Bey, I., Jacob, D. J., Yantosca, R. M., Logan, J. A., Field, B. D., Fiore, A. M., Li, Q.,
712 Liu, H., Mickley, L. J., and Schultz, M. G.: Global modeling of tropospheric

713 chemistry with assimilated meteorology: Model description and evaluation, J.
714 Geophys. Res., 106(D19), 23,073–23,096, 2001.

715 Behera, S. N., Sharma, M., Aneja, V. P., and Balasubramanian, R.: Ammonia in the
716 atmosphere: a review on emission sources, atmospheric chemistry and deposition
717 on terrestrial bodies, Environ. Sci. Pollut. Res., 20, 8092–8131,
718 doi:10.1007/s11356-013-2051-9, 2013.

719 Cape, J.N., Van Dijk, N., and Tang, Y.S.: Measurement of dry deposition to bulk
720 collectors using a novel flushing sampler. J. Environ. Monit., 11, 353-358,
721 doi: 10.1039/B813812E, 2009.

722 Chan, C.K. and Yao, X.H.: Air pollution in mega cities in China, Atmos. Environ., 42,
723 1–42, doi: 10.1016/j.atmosenv.2007.09.003, 2008.

724 Chen, D., Wang, Y. X., McElroy, M. B., He, K., Yantosca, R. M., and Le Sager, P.:
725 Regional CO pollution in China simulated by high-resolution nested-grid
726 GEOS-Chem model, Atmos. Chem. Phys., 11, 3825-3839, 2009.

727 Chen, X. Y. and Mulder, J.: Atmospheric deposition of nitrogen at five subtropical
728 forested sites in South China, Sci. Total Environ., 378, 317–330, doi:
729 10.1016/j.scitotenv.2007.02.028, 2007.

730 Clark, C. M. and Tilman, D.: Loss of plant species after chronic low-level nitrogen
731 deposition to prairie grasslands, Nature, 451, 712–715, doi:10.1038/nature06503,
732 2008.

733 Clarke, J. F., Edgerton, E. S., and Martin, B. E.: Dry deposition calculations for the
734 Clean Air Status and Trends Network, Atmos. Environ., 31, 3667-3678, 1997.

735 CSY (China Statistical Yearbook), 2007-2014. Available at: <http://www.stats.gov.cn>.

736 Cui, J., Zhou, J., Peng, Y., He, Y. Q., Yang, H., Mao, J. D., Zhang, M. L., Wang, Y. H.,
737 and Wang, S. W.: Atmospheric wet deposition of nitrogen and sulfur in the
738 agroecosystem in developing and developed areas of Southeastern China, Atmos.
739 Environ., 89, 102–108, doi:10.1016/j.atmosenv.2014.02.007, 2014.

740 Dentener, F., Drevet, J., Lamarque, J. F., Bey, L., Eickhout, B., Fiore, A.
741 M. Hauglustaine, D., Horowitz, L. W., Krol, M., and Kulshrestha, U. C. :
742 Nitrogen and sulfur deposition on regional and global scales: a multimodel

743 evaluation, *Global Biogeochemical Cy.*, 20, GB4003, doi: 10.1029/2005GB002672,
744 2006.

745 Dore, A.J., Kryza, M., Hall, J. Hallsworth, S., Keller, V., Vieno, M. and Sutton, M.A.:
746 The influence of model grid resolution on estimation of national scale nitrogen
747 deposition and exceedance of critical loads, *Biogeosciences*, 9, 1597-1609, 2012.

748 Du, E. Z., Vries, W. D., Galloway, J. N., Hu, X. Y., and Fang, J. Y.: Changes in wet
749 nitrogen deposition in the United States between 1985 and 2012, *Environ. Res.*
750 *Lett.*, 9, 095004, doi:10.1088/1748-9326/9/9/095004, 2014.

751 EEA: Air Quality in Europe-2011 Report. Technical Report 12/2011. EEA,
752 Copenhagen, 2011.

753 Ellis, R. A., Jacob, D. J., Sulprizio, M. P., Zhang, L., Holmes, C. D., Schichtel, B. A.,
754 Blett, T., Porter, E., Pardo, L. H., and Lynch, J. A.: Present and future nitrogen
755 deposition to national parks in the United States: critical load exceedances, *Atmos.*
756 *Chem. Phys.*, 13, 9083-9095, doi:10.5194/acp-13-9083-2013, 2013.

757 Endo, T., Yagoh, H., Sato, K., Matsuda, K., Hayashi, K., Noguchi, I., and Sawada, K.:
758 Regional characteristics of dry deposition of sulfur and nitrogen compounds at
759 EANET sites in Japan from 2003 to 2008, *Atmos. Environ.*, 45,
760 1259–1267, doi:10.1016/j.atmosenv.2010.12.003, 2010.

761 Erisman, J. W., Vermeulen, A., Hensen, A., Flechard, C., Dammgén, U., Fowler, D.,
762 Sutton, M., Grunhage, L., and Tuovinen, J.P.: Monitoring and modelling of
763 biosphere/atmosphere exchange of gases and aerosols in Europe, *Environ. Pollut.*,
764 133, 403–413, doi:10.1016/j.envpol.2004.07.004, 2005.

765 Flechard, C. R., Nemitz, E., Smith, R. I., Fowler, D., Vermeulen, A. T., Bleeker, A.,
766 Erisman, J. W., Simpson, D., Zhang, L., Tang, Y. S., and Sutton, M. A.: Dry
767 deposition of reactive nitrogen to European ecosystems: a comparison of inferential
768 models across the NitroEurope network, *Atmos. Chem. Phys.*, 11,
769 2703–2728, doi:10.5194/acp-11-2703-2011, 2011.

770 Fowler, D., Coyle, M., Skiba, U., Sutton, M. A., Cape, J. N., Reis, S., Sheppard, L. J.,
771 Jenkins, A., Grizzetti, B., Galloway, J. N., Vitousek, P., Leach, A., Bouwman, A. F.,
772 Butterbach-Bahl, K., Dentener, F., Stevenson, D., Amann, M., and Voss, M.: The

773 global nitrogen cycle in the twenty-first century, *Phil. Trans. R. Soc. B*, 368,
774 20130164, doi:10.1098/rstb.2013.0164, 2013.

775 Galloway, J. N., Dentener, F. J., Capone, D. G., Boyer, E. W., Howarth, R. W.,
776 Seitzinger, S. P., Asner, G. P., Cleveland, C. C., Green, P. A., Holland, E. A., Karl,
777 D. M., Michaels, A. F., Porter, J. H., Townsend, A. R., and Vorosmarty, C. J.:
778 Nitrogen cycles: past, present, and future, *Biogeochem.*, 70, 153–226, 2004.

779 Galloway, J. N., Townsend, A. R., Erisman, J. W., Bekunda, M., Cai, Z., Freney, J. R.,
780 Martinelli, L. A., Seitzinger, S. P., and Sutton, M. A.: Transformation of the
781 Nitrogen Cycle: Recent trends, questions, and potential solutions, *Science*, 320,
782 889–892, 2008.

783 Galloway, J. N., Leach, A. M., Bleeker, A., and Erisman, J. W.: A chronology of
784 human understanding of the nitrogen cycle, *Phil. Trans. R. Soc. B*, 368, 20130120,
785 doi:10.1098/rstb.2013.0120, 2013.

786 Goulding, K. W. T., Bailey, N. J., Bradbury, N. J., Hargreaves, P., Howe, M., Murphy,
787 D. V., Poulton, P. R., and Willison, T. W.: Nitrogen deposition and its contribution
788 to nitrogen cycling and associated soil processes, *New Phytol.*, 139, 49–58, 1998.

789 Gu, B. J., Ge, Y., Ren, Y., Xu, B., Luo, W. D., Jiang, H., Gu, B. H., and Chang, J.:
790 Atmospheric reactive nitrogen in China: Sources, recent trends, and damage costs,
791 *Environ. Sci. Technol.*, 46, 9240–9247, doi:10.1021/es301446g, 2012.

792 Gu, B. J., Sutton, M. A., Chang, S. X., Ge, Y., and Jie, C.: Agricultural ammonia
793 emissions contribute to China's urban air pollution, *Front. Ecol. Environ.*, 12,
794 265–266, doi:10.1890/14.WB.007, 2014.

795 Holland, E. A., Braswell, B. H., Sulzman, J., and Lamarque, J. F.: Nitrogen deposition
796 onto the United States and Western Europe: synthesis of observations and models,
797 *Ecol. Appl.*, 15, 38–57, 2005.

798 Hu, H., Yang, Q., Lu, X., Wang, W., Wang, S., and Fan, M.: Air pollution and control
799 in different areas of China. *Crit. Rev. Environ. Sci. Technol.*, 40, 452–518,
800 doi:10.1080/10643380802451946, 2010.

801 Huang, X., Song, Y., Li, M. M., Li, J. F., Huo, Q., Cai, X. H., Zhu, T., Hu, M., and
802 Zhang, H. S.: A high-resolution ammonia emission inventory in China, *Global*

803 Biogeochem. Cy., 26, GB1030, doi:10.1029/2011GB004161, 2012.

804 Huang, Y. L., Lu, X. X., and Chen, K.: Wet atmospheric deposition of nitrogen: 20
805 years measurement in Shenzhen City, China, *Environ. Monit. Assess.*, 185, 113–
806 122, doi: 10.1007/s10661-012-2537-9, 2013.

807 Jia, Y. L., Yu, G. R., He, N. P., Zhan, X. Y., Fang, H. J., Sheng, W. P., Zuo, Y., Zhang,
808 D. Y., and Wang, Q. F.: Spatial and decadal variations in inorganic nitrogen wet
809 deposition in China induced by human activity. *Sci. Rep.*, 4, 3763, doi:
810 10.1038/srep03763, 2014.

811 Jickells, T., Baker, A. R., Cape, J. N., Cornell, S.E., and Nemitz, E.: The cycling of
812 organic nitrogen through the atmosphere. *Philos. Trans. R. Soc. B* 368, 20130115,
813 doi:org/10.1098/rstb.2013.0115, 2013.

814 Li, Y. E. and Lin, E. D.: Emissions of N₂O, NH₃ and NO_x from fuel combustion,
815 industrial processes and the agricultural sectors in China. *Nutr. Cycl. Agroecosys.*,
816 57, 99–106, 2000.

817 Liu, X. J., Song, L., He, C. E., and Zhang, F. S.: Nitrogen deposition as an important
818 nutrient from the environment and its impact on ecosystems in China, *J. Arid Land*,
819 2, 137–143, 2010.

820 Liu, X. J., Duan, L., Mo, J. M., Du, E., Shen, J. L., Lu, X. K., Zhang, Y., Zhou, X. B.,
821 He, C. E., and Zhang, F. S.: Nitrogen deposition and its ecological impact in China:
822 An overview, *Environ. Pollut.*, 159, 2251–2264, doi:10.1016/j.envpol.2010.08.002,
823 2011.

824 Liu, X. J., Zhang, Y., Han, W. X., Tang, A., Shen, J. L., Cui, Z. L., Vitousek, P.,
825 Erisman, J. W., Goulding, K., Christie, P., Fangmeier, A., and Zhang, F. S.:
826 Enhanced nitrogen deposition over China, *Nature*, 494, 459–462,
827 doi:10.1038/nature11917, 2013.

828 Liu, X. J., Xu, W., Pan, Y. P., and Du, E. Z.: Liu et al. suspect that Zhu et al. (2015)
829 may have underestimated dissolved organic nitrogen (N) but overestimated total
830 particulate N in wet deposition in China, *Sci. Total Environ.*, 520, 300–301,
831 doi.org/10.1016/j.scitotenv.2015.03.004, 2015.

832 Loubet, B., Asman, W. A. H., Theobald, M. R., Hertel, O., Tang, S. Y., Robin, P.,

833 Hassouna, M., Dämmgen, U., Genermont, S., Cellier, P., and Sutton, M. A.:
834 Ammonia deposition near hot spots: processes, models and monitoring methods. In:
835 Sutton MA, Reis S, Baker SMH, editors. Atmospheric ammonia: detecting
836 emission changes and environmental impacts. Netherlands: Springer;
837 205-251.,2008.

838 Lü, C. Q. and Tian, H. Q.: Spatial and temporal patterns of nitrogen deposition in
839 China: Synthesis of observational data, *J. Geophys. Res.*, 112, D22S05,
840 doi:10.1029/2006JD007990, 2007.

841 Lü, C. Q. and Tian, H. Q.: Half-century nitrogen deposition increase across China: A
842 gridded time-series data set for regional environmental assessments. *Atmos.*
843 *Environ.*, 97, 68-74, 2014.

844 Luo, X. S., Liu, P., Tang, A. H., Liu, J. Y., Zong, X. Y., Zhang, Q., Kou, C. L., Zhang,
845 L. J., Fowler, D., Fangmeier, A., Christie, P., Zhang, F. S., and Liu, X. J.: An
846 evaluation of atmospheric Nr pollution and deposition in North China after the
847 Beijing Olympics, *Atmos. Environ.*, 74, 209–216,
848 doi:10.1016/j.atmosenv.2013.03.054, 2013.

849 Maston, P., Lohse, K. A., and Hall, S. J.: The globalization of nitrogen deposition:
850 Consequences for terrestrial ecosystems, *Ambio*, 31, 113–119, 2002.

851 MEPC (Ministry of Environmental Protection of the People’s Republic of China):
852 China’s environment and data center. www.zhb.gov.cn/. Viewed 23 April 2014,
853 2014

854 Pan, Y. P., Wang, Y. S., Tang, G. Q., and Wu, D.: Wet and dry deposition of
855 atmospheric nitrogen at ten sites in Northern China. *Atmos. Chem. Phys.*, 12,
856 6515-6535, doi:10.5194/acp-12-6515-2012, 2012.

857 Reche, C., Viana, M., Pandolfi, M., Alastuey, A., Moreno, T., Amato, F., Ripoll, A.,
858 and Querol, X.: Urban NH₃ levels and sources in a Mediterranean environment.
859 *Atmos. Environ.*, 57:153–164, doi:10.1016/j.atmosenv.2012.04.021, 2012.

860 Richter, D. D., Burrows, J. P., N Nüß, H., Granier, C., and Niemeier, U.: Increase in
861 tropospheric nitrogen dioxide over China observed from space, *Nature* 437,
862 129–132, 2005.

863 Seinfeld, J. and Pandis, S.: Atmospheric Chemistry and Physics: From Air Pollution
864 to Climate Change, John Wiley and Sons, 2nd Edition, 1203 pp., 2006.

865 Schwede, D., Zhang, L., Vet, R., and Lear, G.: An intercomparison of the deposition
866 models used in the CASTNET and CAPMoN networks, *Atmos. Environ.*, 45,
867 1337–1346, doi:10.1016/j.atmosenv.2010.11.050, 2011.

868 Shen, J. L., Tang, A. H., Liu, X. J., Fangmeier, A., Goulding, K. T. W., and Zhang, F.
869 S.: High concentrations and dry deposition of reactive nitrogen species at two sites
870 in the North China Plain, *Environ. Pollut.*, 157, 3106–3113,
871 doi:10.1016/j.envpol.2009.05.016, 2009.

872 Simpson, D., Fagerli, H., Jonson, J.E., Tsyro, S., Wind, P., and Tuovinen, J. P.:
873 Trans-boundary Acidification and Eutrophication and Ground Level Ozone in
874 Europe: Unified EMEP Model Description, EMEP Status Report 1/2003 Part I,
875 EMEP/MSC-W Report, The Norwegian Meteorological Institute, Oslo, Norway,
876 2003.

877 Skeffington, R. A. and Hill, T. J.: The effects of a changing pollution climate on
878 throughfall deposition and cycling in a forested area in southern England, *Sci. Total*
879 *Environ.*, 434, 28–38, doi:10.1016/j.scitotenv.2011.12.038, 2012.

880 Sickles, J. E. and Shadwick, D. S.: Air quality and atmospheric deposition in the
881 eastern US: 20 years of change, *Atmos. Chem. Phys.*, 15, 173–197, doi:
882 10.5194/acp-15-173-2015, 2015.

883 Sutton, M.A., Pitcairn, C.E.R., and Fowler, D.: The exchange of ammonia between
884 the atmosphere and plant communities. *Adv. Ecol. Res.*, 24, 301-393,
885 doi:10.1016/S0065-2504(08)60045-8, 1993.

886 Sutton, M. A., Burkhardt, J. K., Guerin, D., Nemitz, E., and Fowler, D.: Development
887 of resistance models to describe measurements of bi-directional ammonia
888 surface-atmosphere exchange, *Atmos. Environ.*, 32, 473–480,
889 doi:10.1016/S1352-2310(97)00164-7, 1998.

890 Sutton, M. A., Tang, Y. S., Miners, B., and Fowler, D.: A new diffusion denuder
891 system for long-term, regional monitoring of atmospheric ammonia and ammonium,
892 *Water Air Soil Poll. Focus*, 1, 145–156, 2001.

893 Tang, Y. S., Simmons, I., van Dijk, N., Di Marco, C., Nemitz, E., Dammgén,
894 U., Gilke, K., Djuricic, V., Vidic, S., Gliha, Z.: European scale application of
895 atmospheric reactive nitrogen measurements in a low-cost approach to infer dry
896 deposition fluxes. *Agr. Ecosyst. Environ.*, 133, 183–195, doi:
897 10.1016/j.agee.2009.04.027, 2009.

898 Torseth, K., Aas, W., Breivik, K., Fjaeraa, A. M., Fiebig, M., Hjellbrekke, A. G.,
899 Myhre, C. L., Solberg, S., Yttri, K. E.: Introduction to the European Monitoring and
900 Evaluation Programme (EMEP) and observed atmospheric composition change
901 during 1972–2009, *Atmos. Chem. Phys.*, 12, 5447–5481, doi:
902 10.5194/acp-12-5447-2012, 2012.

903 Vitousek, P. M., Aber, J. D., Howarth, R. W., Likens, G. E., Matson, P. A., Schindler,
904 D. W., Schlesinger, W. H., and Tilman, D. G.: Human alteration of the global
905 nitrogen cycle: Sources and consequences, *Ecol. Appl.*, 7, 737–750, 1997.

906 Vet, R., Artz, R. S., Carou, S., Shaw, M., Ro, C-U., Aas, W., Baker, A., and 14 authors:
907 A global assessment of precipitation chemistry and deposition of sulfur, nitrogen,
908 sea salt, base cations, organic acids, acidity and pH, and phosphorus, *Atmos.*
909 *Environ.*, 93, 3–100, doi:10.1016/j.atmosenv.2013.10.060, 2014.

910 Wang, S. X., Xing, J., Zhao, B., Jang, C., and Hao, J. M.: Effectiveness of national air
911 pollution control policies on the air quality in metropolitan areas of China, *J.*
912 *Environ. Sci.*, 26, 13–22, doi: 10.1016/S1001-0742(13)60381-2, 2014.

913 Wang, T., Nie, W., Gao, J., Xue, L. K., Gao, X. M., Wang, X. F., Qiu, J., Poon, C. N.,
914 Meinardi, S., Blake, D., Wang, S. L., Ding, A. J., Chai, F. H., Zhang, Q. Z., and
915 Wang, W. X.: Air quality during the 2008 Beijing Olympics: secondary pollutants
916 and regional impact, *Atmos. Chem. Phys.*, 16, 7603–7615,
917 doi:10.5194/acp-10-7603-2010, 2010.

918 Wesely, M. L.: Parameterization of surface resistances to gaseous dry deposition in
919 regional-scale numerical-models, *Atmos. Environ.*, 23, 1293-1304, 1989.

920 Xing, J., Pleim, J., Mathur, R., Pouliot, G., Hogrefe, C., Gan, C. M., Wei, C.:
921 Historical gaseous and primary aerosol emissions in the United States from 1990 to
922 2010, *Atmos. Chem. Phys.*, 13, 7531–7549, doi: 10.5194/acp-13-7531-2013, 2013.

923 Yu, W. T., Jiang, C. M., Ma, Q., Xu, Y. G., Zou, H., and Zhang, S. C.: Observation of
924 the nitrogen deposition in the lower Liaohe River Plain, Northeast China and
925 assessing its ecological risk, *Atmos. Res.*, 101, 460–468,
926 doi:10.1016/j.atmosres.2011.04.011, 2011.

927 Zhan, X., Yu, G., He, N., Jia, B., Zhou, M., Wang, C., Zhang, J., Zhao, G., Wang, S.,
928 Liu, Y., and Yan, J.: Inorganic nitrogen wet deposition: Evidence from the
929 North-South Transect of Eastern China, *Environ. Pollut.*, 204, 1–8, doi:
930 10.1016/j.envpol.2015.03.016, 2015.

931 Zhang, F. S., Wang, J. Q., Zhang, W. F., Cui, Z. L., Ma, W. Q., Chen, X. P., and Jiang,
932 R. F.: Nutrient use efficiency of major cereal crops in China and measures for
933 improvement. *Acta. Pedologia Sinica*, 45, 915–924, 2008a (in Chinese with English
934 abstract).

935 Zhang, G. Z., Pan, Y. P., Tian, S. L., Cheng, M. T., Xie, Y. Z., Wang, H., and Wang, Y.
936 S.: Limitations of passive sampling technique of rainfall chemistry and wet
937 deposition flux characterization. *Res. Environ. Sci.*, 28, 684-690, doi:10.
938 13198/j.issn.1001-6929.2015.05.03, 2015.

939 Zhang, Y., Liu, X. J., Fangmeier, A., Goulding, K. T. W., and Zhang, F. S.: Nitrogen
940 inputs and isotopes in precipitation in the North China Plain, *Atmos. Environ.*, 42,
941 1436–1448, doi:10.1016/j.atmosenv.2007.11.002, 2008b.

942 Zhang, Y., Dore, A. J., Ma, L., Liu, X. J., Ma, W. Q., Cape, J. N., and Zhang, F. S.:
943 Agricultural ammonia emissions inventory and spatial distribution in the North
944 China Plain, *Environ. Pollut.*, 158, 490–501, doi:10.1016/j.envpol.2009.08.033,
945 2010.

946 Zhang, Y., Song, L., Liu, X. J., Li, W. Q., Lü, S. H., Zheng, L. X., Bai, Z. C., Cui,
947 G. Y., and Zhang, F. S.: Atmospheric organic nitrogen deposition in China. *Atmos.*
948 *Environ.*, 46, 195–204, doi:10.1016/j.atmosenv.2011.09.080, 2012a.

949 Zhang, L., Jacob, D. J., Knipping, E. M., Kumar, N., Munger, J. W., Carouge, C. C.,
950 van Donkelaar, A., Wang, Y. X., and Chen, D.: Nitrogen Deposition to the United
951 States: Distribution, Sources, and Processes, *Atmos. Chem. Phys.*, 12, 4539-4554,
952 doi:10.5194/acp-12-4539-2012, 2012b.

953 Zhang, L. M., Gong, S. L., Padro, J., and Barrie, L.: A size-segregated particle dry
954 deposition scheme for an atmospheric aerosol module, *Atmos. Environ.*, 35 (3),
955 549-560, doi:10.1016/s1352-2310(00)00326-5, 2001.

956 Zhao, Y. H., Zhang, L., Pan, Y. P., Wang, Y. S., Paulot, F., and Henze, D. K.:
957 Atmospheric nitrogen deposition to the northwestern Pacific: seasonal variation and
958 source attribution, *Atmos. Chem. Phys. Discuss.*, 15, 13657-13703,
959 doi:10.5194/acpd-15-13657-2015, 2015.

960 Zhu, J. X., He, N. P., Wang, Q. F., Yan, G. F., Wen, D., Yu, G. R., and Jia, Y. L.: The
961 composition, spatial patterns, and influencing factors of atmospheric wet nitrogen
962 deposition in Chinese terrestrial ecosystems. *Sci. Total Environ.*, 511, 777-785,
963 doi:org/10.1016/j.scitotenv.2014.12.038, 2015.

964

965

966

967

968

969

970

971

972

973

974

975

976

977

978

979

980

981

982 **Figure captions**

983 **Fig. 1.** Geographical distribution of the forty-three monitoring sites in China.

984 **Fig. 2.** Annual mean concentrations of N_r compounds in air (a) and volume-weighted
985 concentrations of inorganic nitrogen species in precipitation (b) at all monitoring sites.

986 **Fig. 3.** Annual mean concentrations of (a) NH_3 ; (b) NO_2 ; (c) HNO_3 ; (d) pNH_4^+ ; (e)
987 pNO_3^- ; and (f) Total N_r : sum of all measured N_r in air and volume-weighted
988 concentrations of NH_4^+ (g); NO_3^- (h) and Total inorganic N (TIN): sum of NH_4^+ and
989 NO_3^- (i) in precipitation at different land use types in six regions.

990 **Fig. 4.** Annual mean concentrations and deposition fluxes of N_r compounds at
991 different land use types across China: concentrations in air (a); volume-weighted
992 concentrations in precipitation (b); dry N deposition fluxes (c); wet/bulk N deposition
993 fluxes (d). The number of sites with the same land use type can be found in Table S1
994 in the Supplement. Error bars are standard errors of means.

995 **Fig. 5.** Annual deposition flux of various N_r species at the forty-three selected sites in
996 China: (a) dry deposition flux; (b) wet/bulk deposition flux; (c) total deposition flux.
997 Yellow dots denote ratios of reduced N to oxidized N in dry deposition (a), NH_4^+ -N
998 to NO_3^- -N in wet/bulk deposition (b) and/or reduced N to oxidized N in total
999 deposition (c) at all sampling sites.

1000 **Fig. 6.** Dry N deposition fluxes of (a) NH_3 ; (b) NO_2 ; (c) HNO_3 ; (d) pNH_4^+ ; (e) pNO_3^- ;
1001 and (f) Total N_r : sum of all measured N_r in dry and wet/bulk N deposition fluxes of
1002 NH_4^+ (g); NO_3^- (h) and Total inorganic N (TIN): sum of NH_4^+ and NO_3^- (i) at
1003 different land use types in the six regions. The number of sites with the same land use
1004 type can be found in Table S1 in the Supplement. Error bars are standard errors of
1005 means.

1006 **Fig. 7.** Contribution of different pathways (dry-deposited N=gaseous N+ particulate N,
1007 wet/bulk-deposited N=precipitation N) to the estimated total N deposition in the six
1008 regions: (a) NC: north China; (b) NE: northeast China; (c) NW: northwest China; (d)
1009 SE: southeast China; (e) SW: southwest China; (f) TP: Tibetan Plateau.

1010 **Fig. 8.** Correlations between annual wet/bulk NH_4^+ -N deposition and annual
1011 volume-weighted concentration of NH_4^+ -N (a) and annual precipitation (b); between
1012 annual wet/bulk NO_3^- -N deposition and annual volume-weighted concentration of
1013 NO_3^- -N (c) and annual precipitation (d).

1014 **Fig. 9.** Spatial variation of atmospheric N deposition flux with emission distribution
1015 in China: (a) NH_3 emission vs. NH_x deposition; (b) NO_x emission vs. NO_y deposition;
1016 (c) relationship of NH_x deposition vs. NH_3 emission; (d) relationship of NO_y
1017 deposition vs. NO_x emission.

1018

1019

1020

1021

1022

1023

1024

1025

1026

1027

1028

1029

1030

1031

1032

1033

1034

1035

1036

1037

1038

1039

1040

1041

1042

1043

1044 **Figure 1**

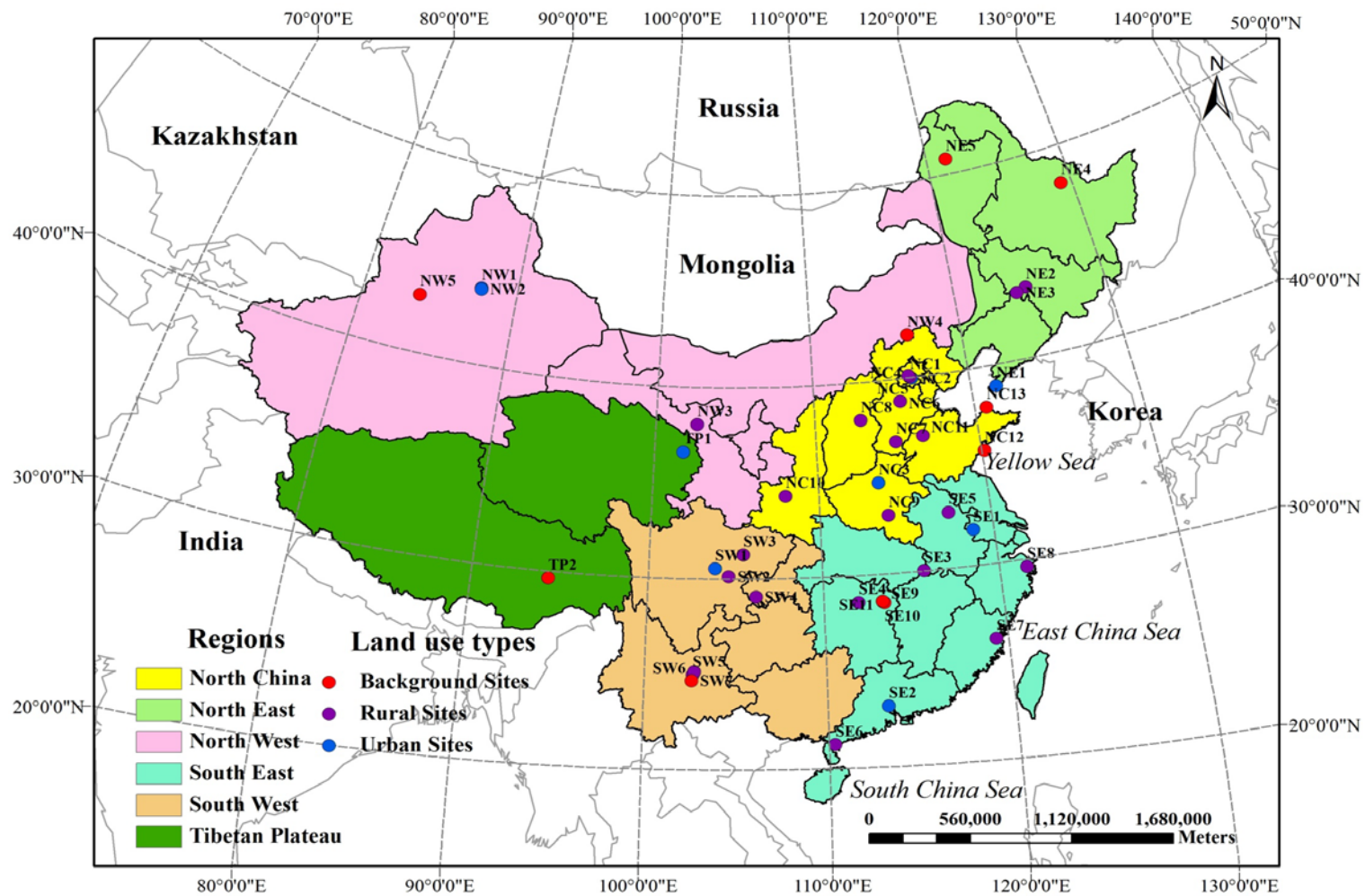
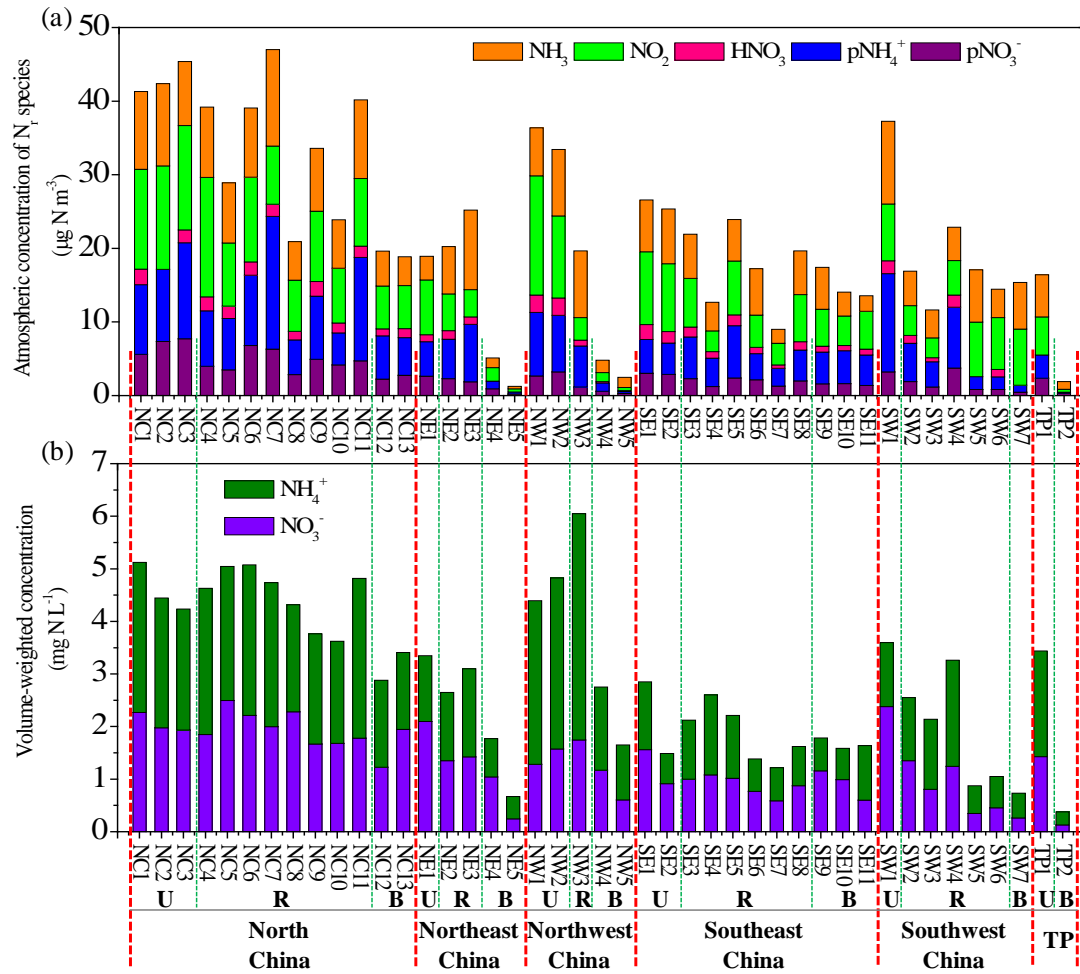


Figure 2



1047

1048

1049

1050

1051

1052

1053

1054

1055

1056

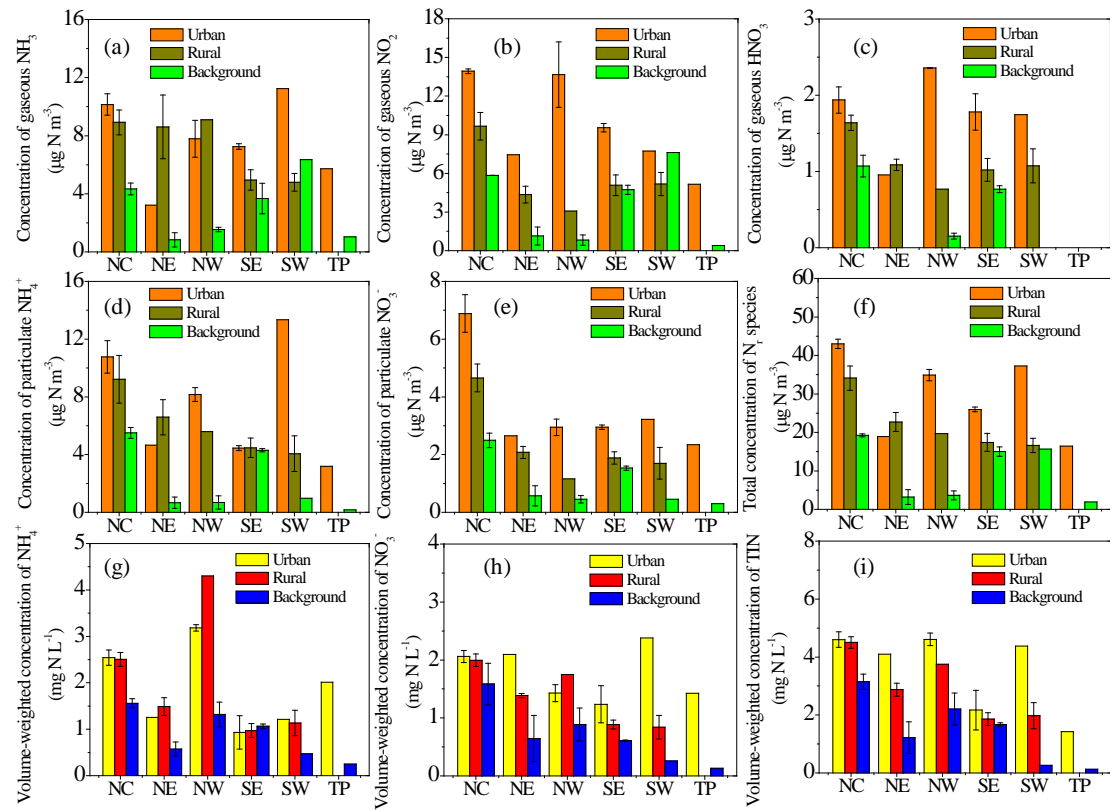
1057

1058

1059

1060

Figure 3



1062

1063

1064

1065

1066

1067

1068

1069

1070

1071

1072

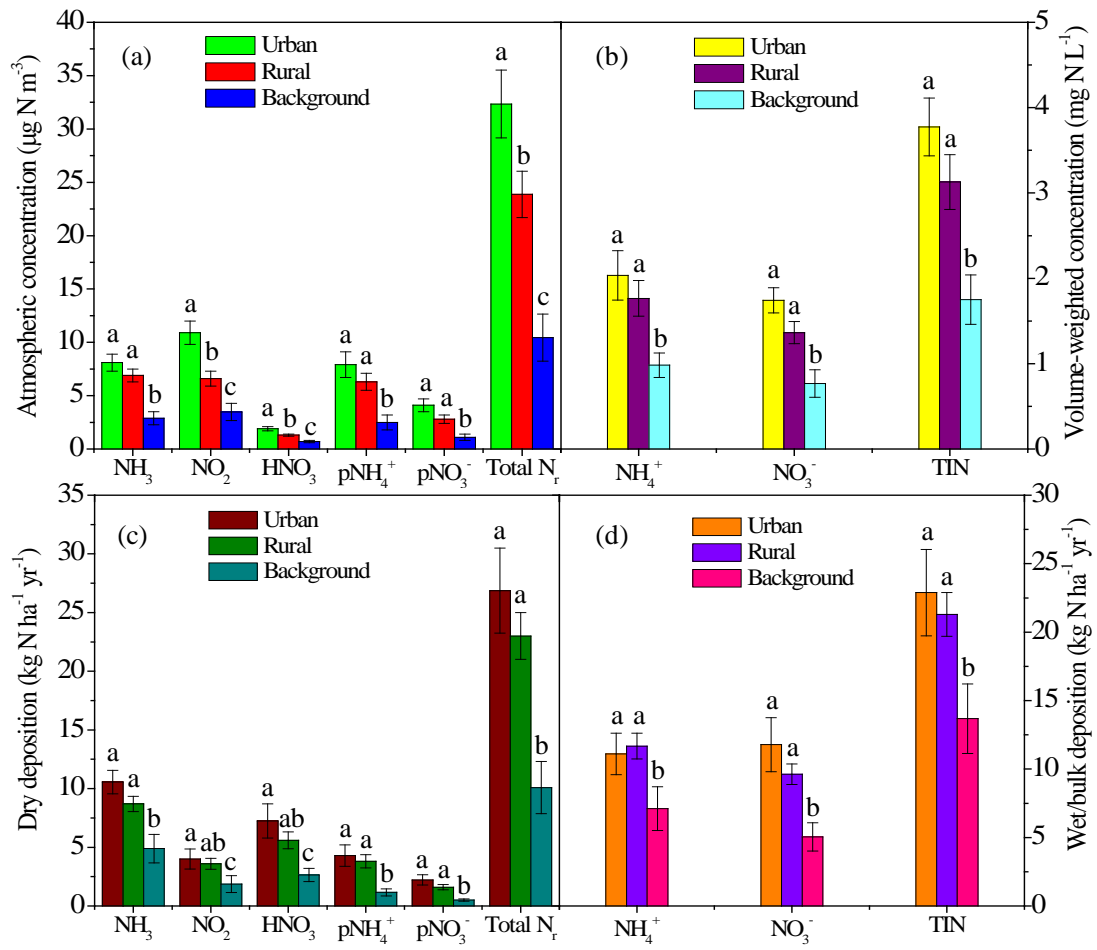
1073

1074

1075

1076

1077



1079

1080

1081

1082

1083

1084

1085

1086

1087

1088

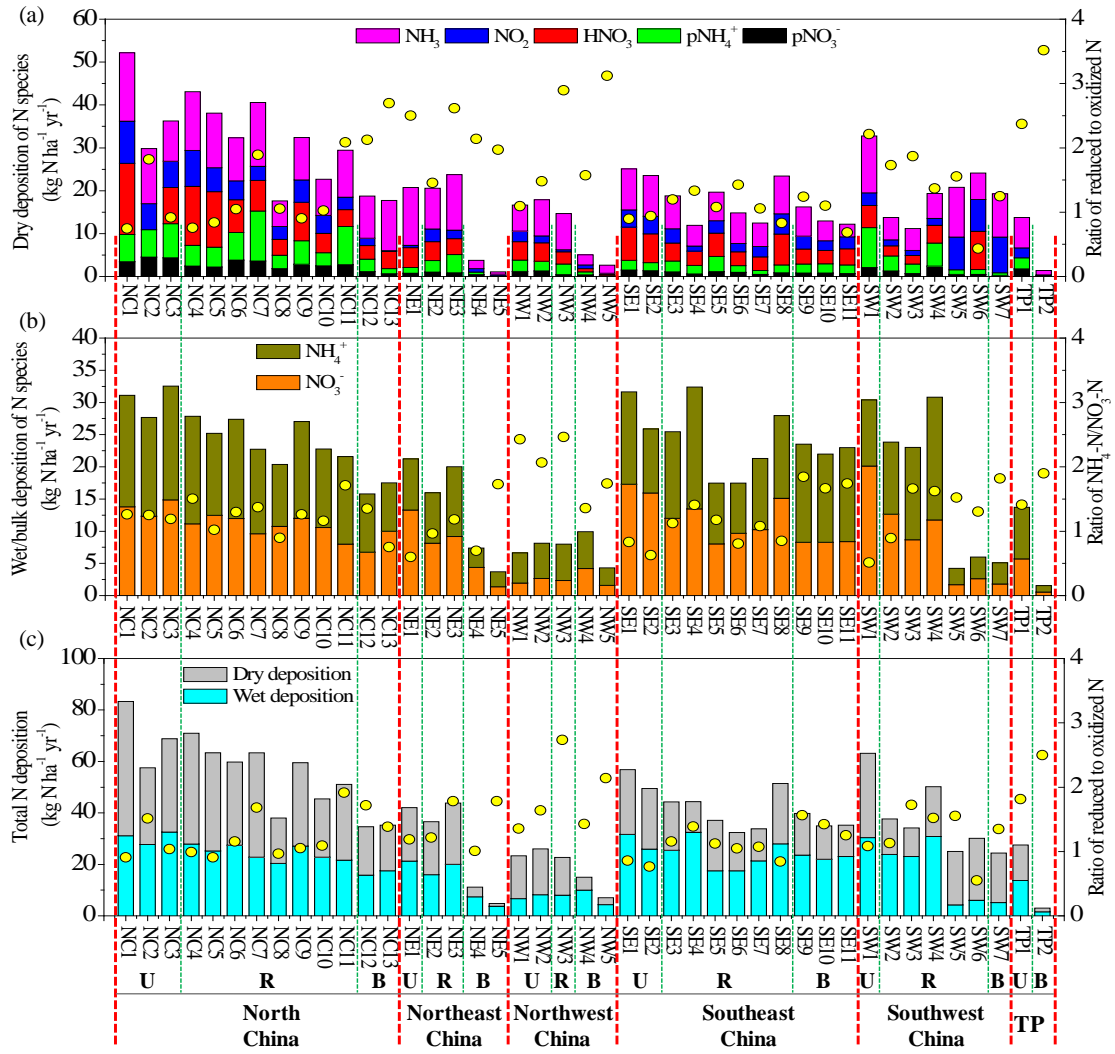
1089

1090

1091

1092

Figure 5



1094

1095

1096

1097

1098

1099

1100

1101

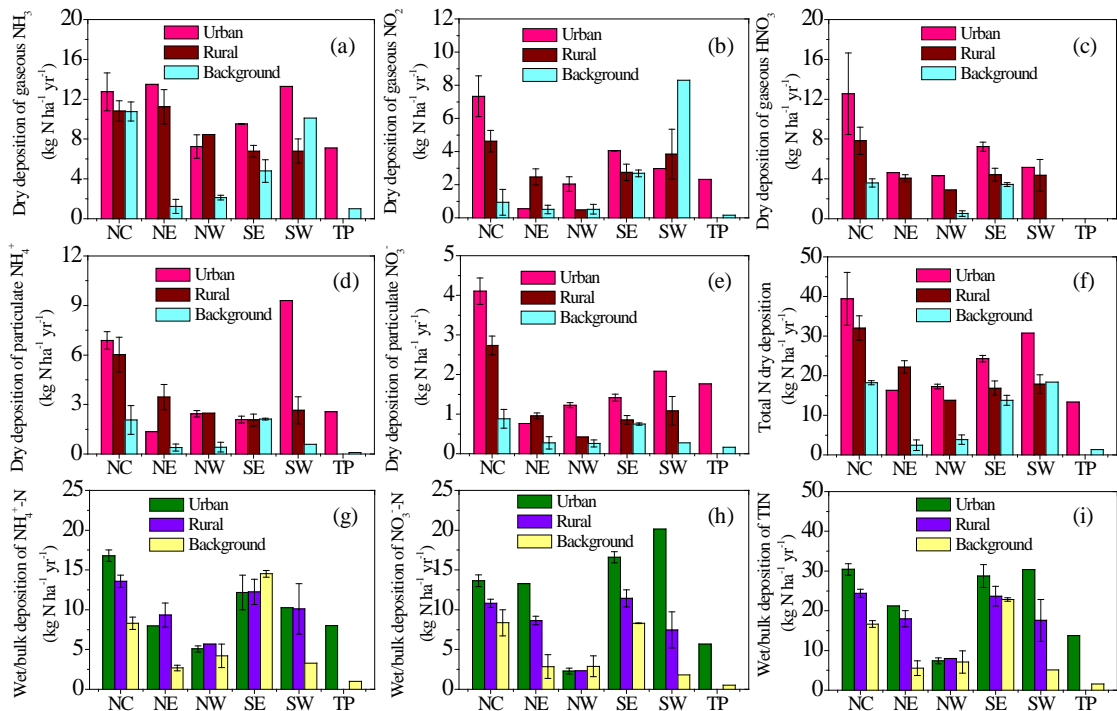
1102

1103

1104

1105

1106 **Figure 6**



1107

1108

1109

1110

1111

1112

1113

1114

1115

1116

1117

1118

1119

1120

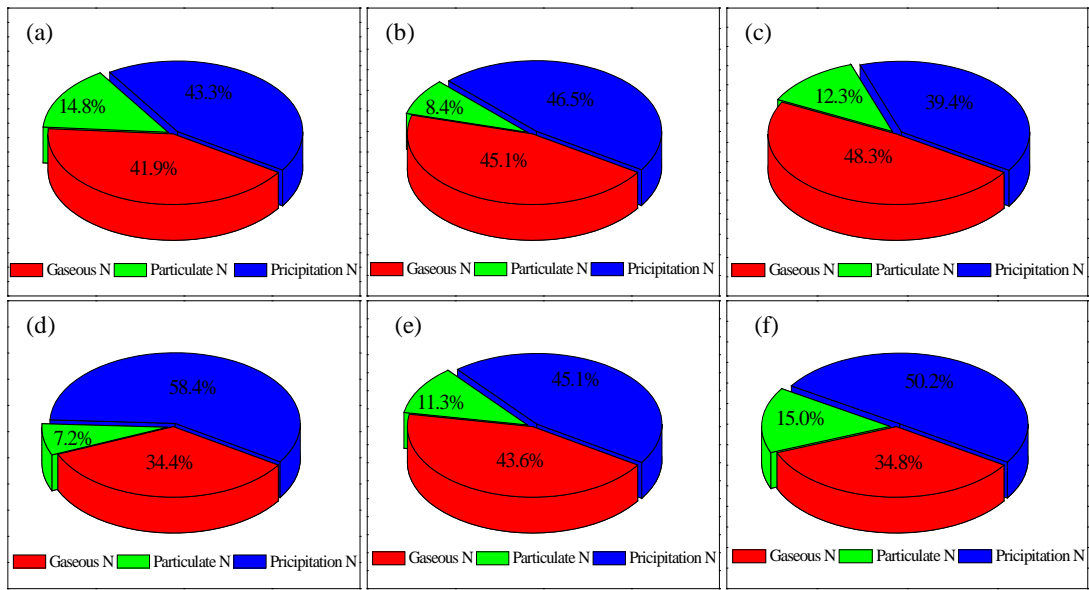
1121

1122

1123

1124

1125 **Figure 7**



1126

1127

1128

1129

1130

1131

1132

1133

1134

1135

1136

1137

1138

1139

1140

1141

1142

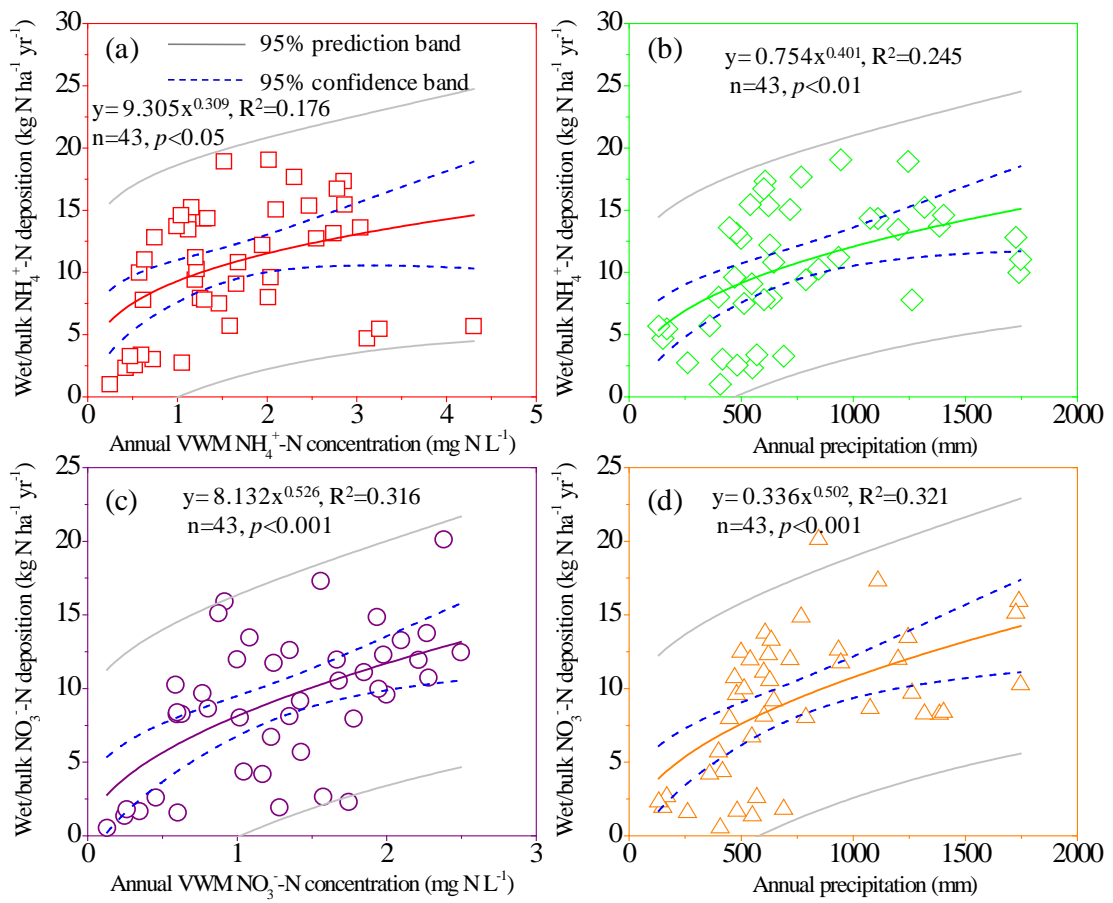
1143

1144

1145

1146

Figure 8



1148

1149

1150

1151

1152

1153

1154

1155

1156

1157

1158

1159

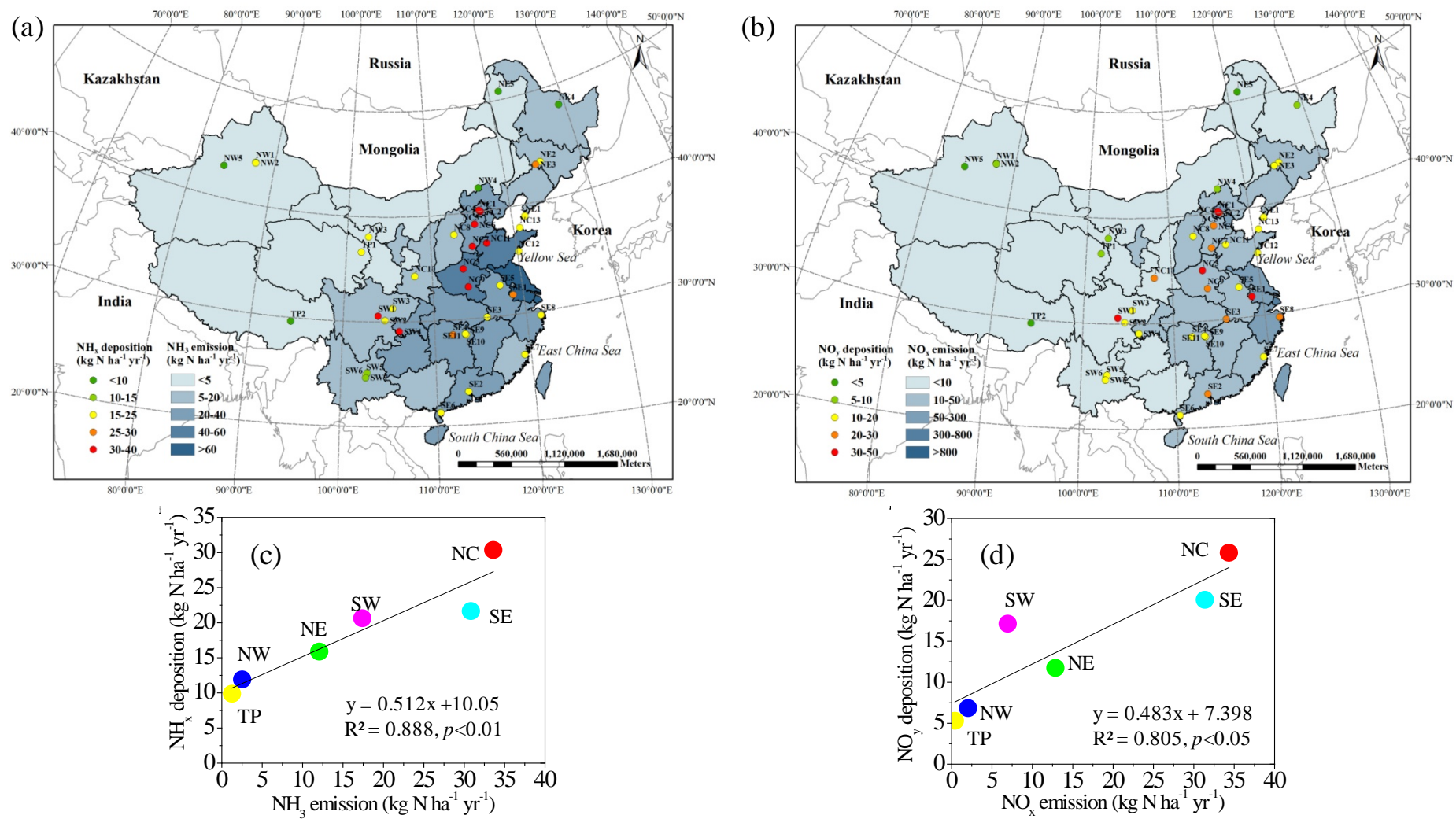
1160

1161

1162

1163

1164



1167 **Table 1.** Comparison of dry, wet (wet/bulk), and total deposition fluxes of N_r compounds between NNDMN in China and 3 networks in other
 1168 countries.

Network	Japan EANET network ^a			CASTNET ^b			EMEP ^c			NADMM ^d			
Number of sites or grids	10 sites			130 sites			2447 grids (0.5° × 0.5°)			33 sites			
Observation period	Apr. 2003-Mar. 2008			Apr. 2006-Dec. 2013			Jan. 2003-Dec. 2007			Aug. 2006-Sep. 2014			
N deposition (kg N ha ⁻¹ yr ⁻¹)	Dry	Wet	Total	Dry	Wet	Total	Dry	Wet	Total	Dry	Wet/bulk	Total	
	Average	3.9	6.6	10.6	3.1	1.3	4.4	3.9	4.8	8.7	18.7	18.2	36.9
	Median	4.1	5.9	11.2	3.0	0.7	4.1	3.7	4.7	8.5	18.7	21.3	36.5
	Max	7.0	15.8	18.2	9.7	10.3	19.6	15.8	16.9	28.0	43.1	32.4	70.9
	Min	1.0	2.1	3.0	0.03	0.1	0.3	0.1	0.6	0.7	1.1	1.5	2.9

1169

1170 ^aThe Japan EANET data are sourced from [Endo et al. \(2011\)](#). Gaseous NO₂ was not included in estimates of dry N deposition.

1171 ^b The CASNET data are available online (<http://www.epa.gov/castnet/>). Gaseous NH₃ was not included in estimates of dry N deposition.

1172 ^cThe EMEP data are sourced from [Endo et al. \(2011\)](#), in which the dry and wet deposition amounts at each grid covering 27 EMEP countries
 1173 were estimated by the unified EMEP models ([Simpson et al., 2003](#)).

1174 ^d Only including the rural and background sites in NNDMN.

1175

1176